

Published in final edited form as:

*Curr Cancer Drug Targets*. 2010 March ; 10(2): 242–267.

## The Biology of the Sodium Iodide Symporter and its Potential for Targeted Gene Delivery

M. Hingorani<sup>1</sup>, C. Spitzweg<sup>2</sup>, G. Vassaux<sup>3</sup>, K. Newbold<sup>4</sup>, A. Melcher<sup>5</sup>, H. Pandha<sup>6</sup>, R. Vile<sup>7</sup>, and K. Harrington<sup>1,\*</sup>

<sup>1</sup>The Institute of Cancer Research, 237 Fulham Road, London, SW3 6JB, UK

<sup>2</sup>Medizinische Klinik II, Klinikum Gross-hadern, 81377 Munich, Germany

<sup>3</sup>Inserm, CHU Hotel Dieu, Nantes, France

<sup>4</sup>Thyroid Unit, The Royal Marsden Hospital, London, UK

<sup>5</sup>Leeds Institute of Molecular Medicine, University of Leeds, Leeds, UK

<sup>6</sup>Postgraduate Medical School, University of Surrey, Surrey, UK

<sup>7</sup>Molecular Medicine Program, Mayo Clinic, Rochester, MN55902, USA

### Abstract

The sodium iodide symporter (NIS) is responsible for thyroidal, salivary, gastric, intestinal and mammary iodide uptake. It was first cloned from the rat in 1996 and shortly thereafter from human and mouse tissue. In the intervening years, we have learned a great deal about the biology of NIS. Detailed knowledge of its genomic structure, transcriptional and post-transcriptional regulation and pharmacological modulation has underpinned the selection of NIS as an exciting approach for targeted gene delivery. A number of *in vitro* and *in vivo* studies have demonstrated the potential of using NIS gene therapy as a means of delivering highly conformal radiation doses selectively to tumours. This strategy is particularly attractive because it can be used with both diagnostic (<sup>99m</sup>Tc, <sup>125</sup>I, <sup>124</sup>I) and therapeutic (<sup>131</sup>I, <sup>186</sup>Re, <sup>188</sup>Re, <sup>211</sup>At) radioisotopes and it lends itself to incorporation with standard treatment modalities, such as radiotherapy or chemoradiotherapy. In this article, we review the biology of NIS and discuss its development for gene therapy.

### INTRODUCTION

The sodium iodide symporter (NIS) belongs to the sodium/solute symporter family [SSF, TC No. 2.A.21 (according to the Transporter Classification system)] or solute carrier family 5 [SCL5A, according to the Online Mendelian Inheritance in Man (OMIM) classification, [www.ncbi.nlm.nih.gov/Omim/](http://www.ncbi.nlm.nih.gov/Omim/)]. This family includes more than 60 members of both prokaryotic and eukaryotic origin, many of which exhibit a high of similarity of sequence and function. Like NIS, many other members of the family drive negatively-charged solutes into the cytoplasm using an electrochemical Na<sup>+</sup> gradient [1]. The eukaryotic members of the family include the three different isoforms of the sodium/glucose co-transporter (SGLT), the sodium/myoinositol co-transporter SMIT (SMIT), the sodium/proline symporter (NPT or

PutP), the sodium/multivitamin transporter (SMVT), the sodium/monocarboxylate transporters (SMCT) and the high-affinity choline transporter.

In recent years, there has been a rapid expansion in our understanding of the biological significance of NIS in thyroid and non-thyroid tissues [1]. The role of NIS in mediating radioiodine uptake underpins the unique clinical status of thyroid cancer as a malignant disease that can be cured by systemic administration of unsealed radioisotope sources [2]. Further research in to the biology of NIS may open the door to effective radioisotopic treatment of thyroid cancer that is iodine non-avid (either *de novo* or as an acquired phenomenon through de-differentiation). In addition, in recent years, there has been a growing appreciation of the potential value of using NIS as a means of achieving therapeutic or imaging goals in non-thyroidal tumour tissues. This work has largely focused on viral vector-mediated delivery of NIS and  $^{131}\text{I}$  to non-thyroid tumour cells in *in vitro* and *in vivo* therapeutic models, but in the last two years NIS expressing vectors have also been administered to patients in early phase clinical trials. In this review we will describe the current state of knowledge of NIS biology and evaluate data relating to therapeutic and imaging studies.

## BIOCHEMICAL AND FUNCTIONAL SIGNIFICANCE OF NIS

Iodide concentration is a characteristic feature of thyroid tissue. As early as 1896, Baumann found that the thyroid gland concentrates iodide by a factor of 20–40 times with respect to plasma under physiological conditions [3]. Iodide is actively transported across the plasma membrane into the cytoplasm of thyroid follicular cells and subsequently translocated passively from the cytoplasm into the follicular lumen. The cell/colloid interface within the follicular lumen is the main site of hormone biosynthesis and involves the coupling of iodide to tyrosine residues on thyroglobulin (Tg) present within the follicular colloid.

NIS is an integral plasma membrane glycoprotein that mediates active transport of iodide into thyroid follicular cells [reviewed in 4] (Fig. 1). The symporter co-transport two sodium ions along with one iodide, with the transmembrane sodium gradient serving as the driving force for iodide uptake. It has previously been shown that on addition of iodide to NIS-expressing cells, an inward steady state current (*i.e.* a net influx of positive charge) is generated leading to depolarization of the membrane. Simultaneous measurements of tracer fluxes and currents revealed that two  $\text{Na}^+$  ions are transported with one anion, demonstrating a 2:1  $\text{Na}^+/\text{I}^-$  stoichiometry [5]. Therefore, the observed inward steady-state current is due to a net influx of  $\text{Na}^+$  ions. NIS functionality is dependent on the electrochemical sodium gradient that is maintained by the ouabain-sensitive  $\text{Na}^+/\text{K}^+$ ATPase pump. The efflux of iodide from the apical membrane to the follicular lumen is driven by pendrin (the Pendred syndrome gene product) and possibly other unknown efflux proteins (apical anion transporters) [6]. Thiocyanate and perchlorate are competitive inhibitors of iodide accumulation in the thyroid due to their similarity in size and charge to iodide ions, although they have different molecular geometries. Perchlorate is 10–100 times more potent than thiocyanate as an inhibitor of iodide accumulation in a variety of *in vivo* and *in vitro* systems. It has also been shown recently that perchlorate is actively transported by NIS, albeit electroneutrally [7].

Iodide organification within the follicular lumen is mediated by the enzyme thyroperoxidase (TPO) that involves oxidation of iodide and its covalent incorporation on tyrosine residues within the Tg backbone followed by the oxidative coupling of iodotyrosines to generate thyroid hormones. More recently, the dual oxidase DUOX2 has been shown to be important in thyroid hormone biosynthesis, as demonstrated by the occurrence of congenital hypothyroidism (total iodide organification defect) in individuals with biallelic inactivating

DUOX2 mutations [8]. The unique property of thyroid follicular cells to trap and concentrate iodide enables imaging as well as effective therapy of differentiated thyroid cancers using radioiodide [2].

## MOLECULAR CHARACTERISATION OF NIS

The molecular characterisation of NIS began in 1996 when Nancy Carrasco's group isolated the cDNA encoding rat NIS (rNIS) by expression cloning in *X. laevis* oocytes, using cDNA libraries derived from FRTL-5 cells (a highly functional rat thyroid-derived cell line) [9]. Based on the expectation that the genomic organisation of human NIS (hNIS) would be highly homologous to rNIS, Smanik *et al.* (1996) isolated cDNA encoding hNIS using primers to the cDNA/rNIS sequence [10]. The cDNA sequence predicted that rNIS was a 618 amino acid protein with a relative molecular mass of 65,196. Elucidation of the secondary structure of NIS protein was facilitated by the generation of a high affinity site-directed polyclonal anti-NIS antibody (Ab) against the last 16 amino acids of the COOH terminus [11]. The current secondary structure model demonstrates 13 transmembrane domains with the NH<sub>2</sub> terminus facing extracellularly and the COOH terminus facing intracellularly. There are three glycosylation sites at positions 225, 485, and 497 of the amino acid sequence. The length of the 13 trans-membrane segments ranges from 20–28 amino acids, except for transmembrane segment V which contains 18 residues [1]. The molecular structure, biochemical and functional activity of NIS are depicted in Fig. (2). Four Leu residues (positions 199, 206, 213, and 220) appear to comprise a putative leucine zipper motif in transmembrane segment VI. This motif could play a role in the oligomerization of subunits in the membrane. Previous freeze fracture electron microscopy studies of *X. laevis* oocytes expressing NIS revealed 9 nm intramembrane particles corresponding to NIS, suggesting that NIS may be an oligomeric protein [5].

The human NIS gene is located on chromosome 19p12–13.2, with an open reading frame of 1929 nucleotides comprising 15 exons and 14 introns that encodes a 643-amino acid protein. hNIS exhibits 84% identity and 93% similarity to rNIS, with the main differences accounted for by a 5 amino acid insertion between the last two hydrophobic domains and a 20 amino acid insertion in the COOH terminus [12].

The high-affinity anti-COOH terminus NIS Ab binds a mature 87 kDa polypeptide and a partially glycosylated 56 kDa polypeptide in permeabilised FRTL-5 cells. It has been previously shown that neither partial nor total lack of N-linked glycosylation impairs activity, stability or targeting of NIS. The hydroxyl group at the  $\beta$  carbon at position 354 (in transmembrane segment IX) is essential for NIS function. Spontaneous mutation consisting of the single amino acid substitution of Pro instead of Thr at position 354 (T354P) is the cause of congenital lack of iodide transport in several patients, often leading to severe hypothyroidism [13]. Hydroxyl groups at serine and threonine residues (Ser 353, Ser 356, Thr 357) in transmembrane segment IX are also essential for NIS activity [14]. Similarly, the presence of an uncharged amino acid residue with a small side-chain at position 395 (normally glycine) is essential for NIS function [15].

## REGULATION OF NIS FUNCTION

### Transcriptional Regulation of NIS

Transcriptional activity of thyroidal NIS is primarily regulated by thyroid stimulating hormone (TSH), via the cyclic adenosine monophosphate (cAMP) pathway [16]. Multiple cAMP pathways, both protein kinase A (PKA)-dependent and -independent, may be involved in the regulation of NIS expression and function. TSH-cAMP-PKA signaling is the central pathway for thyroid proliferation and differentiation and its integrity is essential

for NIS expression. However, the exact mechanism by which PKA promotes NIS expression is still unknown [17]. In FRTL-5 cells, chronic stimulation with TSH downregulates PKA and acute stimulation with cAMP agonists under these conditions results in increased NIS transcriptional activity without PKA activation [18, 19]. The MEK–ERK pathway has been proposed as a PKA-independent pathway, as MEK inhibition partially inhibits cAMP-induced NIS gene transcription (43%) [19]. This pathway seems to be stimulated by TSH through Rap-1 without PKA activation [20, 21]. However, activation of the MAPK pathway in response to TSH/cAMP has not been confirmed by other groups [22, 23]. In addition, the p38 MAPK pathway has been shown to have a pro-stimulatory effect on NIS gene expression that is independent of PKA activation [24].

The phosphatidylinositol 3-kinase (PI3-K) and TGF- $\beta$ /Smad pathways have been shown to have an inhibitory effect on NIS transcription. In FRTL-5 cells, insulin growth factor-1 (IGF-1) inhibits cAMP-induced NIS expression through the PI3K pathway [25]. Furthermore, expression of a Ras mutant that selectively stimulates PI3-K has been shown to markedly decrease TSH-induced NIS expression in WRT rat thyroid cells [26]. TGF- $\beta$  decreases TSH-induced NIS expression and iodide uptake activity in FRTL-5 cells [27, 28]. TGF-induced downregulation of NIS is associated with a decrease in mRNA levels and impaired binding of PAX-8 to the NIS promoter, secondary to the physical interaction between Smad-3 and Pax-8 [29].

The rNIS and hNIS promoters have been studied by several groups [30–34]. The proximal promoter contains a thyroid transcription factor-1 (TTF-1) binding site and a TSH responsive element for interaction with the putative transcription factor NTF-1 (NIS TSH-responsive factor-1) [16]. The DNA sequence upstream of NIS contains two Pax8 binding sites and a degenerate CRE (cAMP responsive element sequence) which are important for full TSH-cAMP-dependent transcription. Similarly, a thyroid-specific, TSH-responsive, far-upstream enhancer has been described in the hNIS gene with a high degree of sequence homology to the rNIS [19, 35]. It contains putative Pax-8 and TTF-1 binding sites and a CRE-like sequence.

TSH is a 30-kDa glycoprotein biosynthesized in the basophilic cells of the adenohypophysis (anterior pituitary) and is the primary hormonal regulator of thyroid function. TSH activation is associated with iodide accumulation in the thyroid. TSH actions are primarily mediated by activation of adenylate cyclase via the GTP binding protein [36, 37]. TSH interacts with the TSH receptor on the basolateral membrane of follicular cells followed by cAMP-mediated biosynthesis of NIS protein [38]. TSH-mediated upregulation of NIS protein expression has been observed *in vivo* [11]. Furthermore, NIS mRNA expression is upregulated by goitrogenic treatments (eg, propylthiouracil (PTU)) that elevate circulating TSH levels *in vivo* [39].

Levy *et al.* (1997) studied the biogenesis of NIS by *in vivo* labeling experiments with [<sup>35</sup>S]-methionine/cysteine followed by immunoprecipitation with high affinity anti-NIS Ab in FRTL-5 cells [11]. They showed that NIS is initially synthesized as a precursor protein that is immediately core-glycosylated in the endoplasmic reticulum at three Asp residues (225, 485, 497) [40]. Further studies have shown that the precursor protein is a 56 kDa polypeptide whose maturation into full length 87 kDa polypeptide is first observed at about 1 hour and is completed at 3 hours after initial TSH stimulation [41]. After TSH withdrawal, a reversible reduction of both intracellular cAMP levels and iodide uptake activity are observed in thyroid cell lines [24]. However, NIS protein has an unusually long half-life and remains detectable 10 days after TSH deprivation [41–43]. Riedel *et al.* (2001) have reported the half-life of NIS protein to be approximately 5 days in the presence and 3 days in the absence of TSH stimulation [41].

## Post-Transcriptional Regulation of NIS

For active iodide transport to occur, NIS must be expressed, targeted and retained in the appropriate plasma membrane surface (i.e. the basolateral surface) in polarized epithelial thyroid cells [44]. In addition to upregulating NIS transcription, TSH also regulates important post-transcriptional events such as the subcellular distribution of NIS. Kogai *et al.* (2000) showed that TSH markedly stimulates NIS mRNA and protein levels in both monolayer and follicle-forming human primary culture thyrocytes. However, significant iodide uptake is observed only in follicle-forming thyrocytes, indicating the importance of cell polarization and spatial organization for functional activity of NIS [45]. Kaminsky *et al.* (1994) reported persistent NIS activity in membrane vesicles prepared from FRTL-5 cells following prolonged TSH withdrawal. Interestingly, no such activity was detected in intact cells in similar conditions [46]. This could be explained by the differential cellular expression of NIS following TSH deprivation. Riedel *et al.* (2001) showed that after 3 days of TSH deprivation, intracellular NIS decreased at a slower rate than the intramembranous fraction, suggesting that NIS molecules in the plasma membrane are redistributed to intracellular compartments in response to TSH withdrawal [41]. In thyroid cancer cells, TSH signaling may be compromised, resulting in NIS retention in intracellular organelles even in the presence of TSH. Previous studies have shown a high frequency of TSH receptor promoter hypermethylation in thyroid cancer, which would cause silencing of the TSH receptor gene and inhibition of functional NIS expression [47].

The mechanism by which TSH regulates the subcellular distribution of NIS is unknown. Phosphorylation has been shown to be implicated in activation and subcellular distribution of several transporters [48–50]. NIS has several consensus sites for kinases, including those for cAMP-dependent protein kinase, PKA and protein kinase C (PKC). Previous studies have shown that NIS is phosphorylated *in vivo*, mainly at the serine residues in the COOH terminus. Furthermore, it is known that NIS phosphorylation is modulated by TSH [41]. However, as yet, there is no conclusive evidence to support the notion that TSH-induced NIS phosphorylation mediates the trafficking and subcellular distribution of NIS.

Although TSH-induced stimulation is essential for efficient NIS trafficking in thyroid tissue, non-thyroidal tissues retain NIS at the plasma membrane in the absence of TSH stimulation - raising the possibility of TSH-independent mechanisms. Furthermore, ectopic expression of NIS in a wide variety of cell lines, ranging from amphibian cells (*X. laevis* oocytes) to mammalian normal (COS cells (green African monkey fibroblasts)) and malignant cells (CHO (Chinese Hamster ovary cells) and LNCaP cells (human prostatic adenocarcinoma)), is associated with efficient functional activity and appropriate targeting to the plasma membrane [1, 51, 52].

NIS contains several sorting signals in its COOH terminus that, in other membrane proteins, are involved in the targeting, retention at and endocytosis from the plasma membrane. NIS contains a PDZ target motif (T/S-X-V/L) at the COOH-terminal tail (T<sup>616</sup> N<sup>617</sup> L<sup>618</sup>) that is a recognition site for PDZ binding proteins [53]. One such protein, LIN-7, recognizes a PDZ target motif in the epithelial  $\gamma$ -aminobutyric transporter and prevents its internalization from the basolateral surface of polarized epithelial cells [54]. NIS also contains a dileucine motif (L<sup>557</sup> L<sup>558</sup>) which may play a role in sorting certain membrane proteins within the cell [44, 47]. The dileucine motif, like tyrosine-based sorting signals, interacts directly with the clathrin-coated machinery [55]. This interaction allows for selective incorporation of integral membrane proteins into coated vesicles that carry proteins to different destinations within the cell. In addition, three acidic dipeptide motifs (E<sup>573</sup> D<sup>574</sup>, E<sup>579</sup> E<sup>580</sup>, E<sup>587</sup> D<sup>588</sup>) are present in the COOH terminus of NIS and these can function as retrieval signals for proteins localized at the cell surface [56, 57] or retention signals in large dense core vesicles, as in the case of the vesicular monoamine transporter [58].

## PROGNOSTIC SIGNIFICANCE OF NIS IN THYROID CANCERS

Radioiodide was first administered in 1942 at the Massachusetts Institute of Technology to patients with Graves' disease [59]. Since then, radioiodide-induced thyroid ablation has become an integral part of the management of thyroid cancer and some non-malignant thyroid disorders. Thyroid cancer patients who are treated with  $^{131}\text{I}$  have a lower mortality compared with those who are not (3% vs 12%). Even patients with metastatic disease at initial presentation can be successfully treated with  $^{131}\text{I}$ , achieving a 10-year survival of over 80%. In contrast, thyroid cancer patients with poor radioiodide uptake, a situation sometimes seen in patients more than 40 years age, have a much poorer prognosis [2].

Studies investigating the molecular mechanisms underlying the variable uptake of iodide observed in thyroid cancer patients have suggested that this may be related to the levels of NIS expression. Smanik *et al.* (1996) reported a much lower level of NIS mRNA expression in thyroid carcinoma (2 papillary, 1 follicular, 1 anaplastic) compared with that in normal thyroid tissue. In addition, they found variable levels of NIS expression in a panel of different papillary carcinoma tissues, which is consistent with the clinical observation of variable response of papillary carcinoma to radioiodine treatment. Furthermore, no NIS mRNA expression was detected in 5 human thyroid carcinoma cell lines that had lost iodide avidity [9]. In a more recent study using a kinetic quantitative RT-PCR method, NIS mRNA expression was shown to be decreased in 40 of 43 thyroid carcinomas (38 papillary and 5 follicular) and in 20 of 24 cold adenomas compared with normal thyroid tissue. On the other hand, NIS mRNA levels were increased in each of 8 toxic adenomas and 5 samples from patients with Graves' disease. In thyroid cancer tissues, a positive correlation was found between the expression levels of NIS, TPO, Tg and thyroid stimulating hormone (TSH) receptor, and higher tumour stages were associated with lower levels of NIS expression [60]. Interestingly, NIS mRNA expression levels have been shown to be reduced in oncogene-transformed rat thyroid cell lines (PC v-*erbA*, PC HaMSV, PC v-*raf* and PC E1A), raising the possibility that oncogene activation may be one of the factors responsible for reduced NIS levels observed in thyroid cancers [61].

Park *et al.* (2000) investigated the correlation of NIS expression between primary and metastatic thyroid tumour tissues. NIS mRNA levels in 23 papillary carcinomas and 7 pairs of primary and lymph node metastatic tissues were evaluated using RT-PCR and ribonuclease protection assay. Three of 23 papillary carcinomas did not express NIS mRNA and the rest showed variable levels of NIS mRNA expression that were lower than those in normal thyroid tissue. Despite NIS expression in the primary tumour, 2 of 6 lymph node metastases did not express NIS mRNA. Levels of NIS mRNA expression in the remaining 4 lymph node metastases were lower than those in the primary tumours. Therefore, no positive correlation was found between NIS expression levels in primary and metastatic sites leading to the conclusion that NIS levels in primary tissue may not be predictive of the response to radioiodide therapy at metastatic sites [62].

Other studies have given a rather different view of the expression levels of NIS in thyroid cancers, suggesting instead that NIS may be expressed or overexpressed but may not be correctly targeted to the cell membrane. Saito *et al.* (1998) used Northern analysis and reported a 2.8-fold increase in mRNA in thyroid tissue from patients with papillary cancer (although there was wide variability in the levels between different individuals) [. Subsequent studies have demonstrated that NIS may be overexpressed in up to 70% of thyroid tumours, but that it is retained within intracellular compartments [64]. The mechanisms responsible for this failure to display NIS correctly at the plasma membrane are, as yet, obscure but may be due to the effects of aberrant oncogene signalling in tumour cells.

## EFFECT OF IODIDE THERAPY ON NIS FUNCTION

Although the function of NIS is to mediate iodide uptake in thyroid tissue, pre-treatment with iodide has been found to have rather complex paradoxical effects on NIS expression and function. Inhibition of thyroid function following administration of large doses of iodide is well-known. Wolff and Chaikoff (1948) first reported that iodide organification in the rat thyroid was blocked when plasma levels of iodide reached a critical high threshold, a phenomenon known as the acute Wolff-Chaikoff effect [65]. In the following year, Raben *et al.* (1949) showed that this could be prevented with the administration of thiocyanate, a competitive inhibitor of iodide uptake, suggesting that the phenomenon was dependent on the intrathyroidal rather than the plasma concentration of iodide [66]. It was further shown that pre-incubation with a TPO inhibitor can abolish the inhibitory effect of iodide, raising the possibility that it is mediated by iodinated intra-cellular compounds, possibly in the form of iodolipids [67]. However, as early as 2 days after onset of the acute effect, an escape or adaptation occurs that leads to gradual normalization of thyroidal functional levels. This escape is mediated by activation of a potential autoregulatory loop and is associated with reduced iodide transport leading to restoration of intracellular iodide levels.

Several studies have now shown that iodide administration is associated with a paradoxical reduction in NIS mRNA and protein levels that, by reducing iodide transport, help to overcome the inhibitory effect of iodide on thyroid hormone synthesis [68–70]. NIS inhibition following iodide therapy is likely to involve both transcriptional and non-transcriptional effects. Furthermore, the half life of the NIS protein is shorter in iodine-treated cells, suggesting increased NIS protein turnover in these cells [68]. Similar to TSH-induced stimulation, the inhibitory effect of iodide on NIS expression and function appears to be thyroid-specific with no evidence of this being a significant phenomenon in non-thyroidal tissues.

## OTHER MODULATORS OF NIS FUNCTION

NIS expression can also be modulated by cytokines produced by infiltrating inflammatory cells and, in some cases, by follicular cells themselves [70]. The thyroidal effects of cytokines (tumour necrosis factor alpha (TNF- $\alpha$ ) and beta (TNF- $\beta$ ), interferon- $\gamma$  (IFN- $\gamma$ ), interleukins 1-alpha (IL-1 $\alpha$ ), 1-beta (IL-1 $\beta$ ), -6 (IL-6) and transforming growth factor-beta (TGF- $\beta$ ) have been evaluated in FRTL-5 cells. Ajjan *et al.* (1998) and Spitzweg *et al.* (1999) reported that TNF- $\alpha$  inhibited TSH-stimulated NIS mRNA expression in FRTL-5 cells [68, 71]. In addition, Pekary *et al.* (1998) reported that TNF-induced inhibition of NIS expression was mediated by the activation of sphingomyelinase, an enzyme that converts sphingomyelin to ceramide in the plasma membrane [27]. Similar effects were observed in human thyroid cells, in which TNF administration was associated with a dose-dependent decrease of cAMP levels and Tg expression [72]. Furthermore, the effect was enhanced when TNFs were combined with IL-1 [68]. Similarly, TGF- $\beta$  inhibits NIS mRNA expression and iodide uptake in a time and dose-dependent manner. TGF- $\beta$  also induces a change in the shape of young FRTL-5 cells from a cuboidal to a flattened stellate morphology. Subsequent ageing of these cells is associated with an increase in spontaneous TGF-expression and secretion that leads to a further reduction of NIS mRNA levels and iodide transport [27, 28]. There is conflicting evidence on the effect of IFN- $\gamma$  on thyroidal NIS expression. Whereas Spitzweg *et al.* (1999) [64] reported that IFN- $\gamma$  had no effect on iodide accumulation or NIS mRNA levels, Ajjan *et al.* (1998) [71] observed that IFN- $\gamma$  at a high concentration (1000 U/ml) down-regulated TSH-stimulated NIS mRNA levels. The latter results were confirmed in an *in vivo* study by Caturegli *et al.* (2000) that reported a severe impairment of thyroid function and a loss of typical follicular structure combined with down-regulation of NIS expression and activity in transgenic mice expressing IFN- $\gamma$  in

the thyroid [73]. Therefore, it seems that the predominant effect of cytokines on TSH-mediated NIS expression is inhibitory.

Previous studies have demonstrated a correlation between the levels of endogenous NIS expression and the degree of differentiation of thyroid tumours (*vide supra*). Oncogenic mutations of BRAF and RAS family genes, as well as RET rearrangements, play an important role in malignant transformation and tumour progression of thyroid cancer. Previous studies have shown that the activation of these oncogenes is associated with a reduction in the mRNA levels of NIS and certain other thyroid-specific genes [74–76]. Moreover, BRAF mutation also leads to impaired targeting and retention of NIS protein at the plasma membrane [77].

In accordance with these observations, several groups have investigated the possible effects of differentiation-inducing agents, including retinoids and troglitazone on endogenous NIS expression. Retinoic acid (RA), a vitamin A derivative, plays a pivotal role in development, differentiation and cell growth. RA action is mediated through two families of nuclear receptors, retinoic acid receptors (RARs) and retinoid X receptors (RXRs). All-trans RA (ATRA), a ‘pan-retinoid’ (non-selective) ligand to all retinoic acid receptor (RAR) isomers, has been shown to induce NIS mRNA in two thyroid cancer cell lines. Interestingly, treatment of FRTL-5 rat thyroid cells with ATRA downregulates NIS mRNA, suggesting differential regulation of NIS expression by RA in normal and malignant thyroid tissues [78]. In a recent study, treatment of an anaplastic thyroid cancer cell line with 1  $\mu$ M of ATRA was associated with a 6.5 fold increase in the level of iodide uptake. Using microarray analysis, the investigators showed that ATRA treatment was associated with differential expression of several genes. More specifically, ATRA increased the expression of BCL3, CSRP3, v-fos, and CDK5 genes and decreased the expression of the FGF12 and IGFBP6 genes [79]. Differential expression of RAR isoforms may be important to predict RA-mediated NIS induction in thyroid cancer. Several clinical trials have been performed using ATRA in order to increase radioiodide uptake and improve clinical outcome of patients with recurrent thyroid cancer [1]. The largest study was carried out on 50 patients with iodide non-avid disease. Twenty-six per cent had a significant increase in radioiodide uptake, but only 16% had reduced tumour volume following  $^{131}$ I administration [80].

Troglitazone is a peroxisome proliferator-activated receptor-gamma (PPAR- $\gamma$ ) agonist that inhibits cell proliferation and induces apoptosis. The chromosomal rearrangement PPAR- $\gamma$ /PAX-8 occurs frequently in follicular thyroid carcinoma and in the follicular variant of papillary thyroid carcinoma. This results in inactivation of PPAR- $\gamma$  function [81, 82]. Troglitazone has been reported to increase NIS mRNA in several thyroid cancer cell lines *in vitro* [83, 84].

Epigenetic modifications, such as histone deacetylation, play an important role in the regulation of gene expression and are likely to be involved in carcinogenesis. Deacetylated histones are generally associated with silencing of gene expression and aberrant acetylation is associated with several solid tumours and haematological malignancies. HDAC inhibitors have been shown to induce differentiation and apoptosis combined with suppression of transformed cell growth both *in vitro* and *in vivo* [85]. Depsipeptide (FR901228) is an HDAC inhibitor that significantly increases NIS mRNA and iodide uptake in several thyroid cancer cell lines (including anaplastic). Interestingly, depsipeptide also induces concomitant expression of TPO, Tg and TTF-1 that leads to restoration of iodide organification and reduced iodide efflux [86, 87]. Valproic acid (VPA) is a class I selective HDAC inhibitor that is also widely used as an anticonvulsant. VPA-induced increase in NIS gene expression and membrane localization combined with enhanced iodide accumulation has been observed in poorly differentiated thyroid cancer cell lines [88]. Furthermore, it has also been reported

that VPA upregulates NIS and Tg mRNA levels by 93–370% in differentiated thyroid cancer (follicular) cell lines [89]. The upregulatory effects of HDAC inhibitors on thyroidal NIS expression, combined with their differentiation and proapoptotic properties, make them strong candidates for further studies to investigate their potential as therapeutic agents in the management of thyroid cancer.

DNA methylation, another epigenetic modification, is a covalent modification of cytosine residues that occurs at the dinucleotide sequence CpG in vertebrates. Nearly, half of all human genes have CpG islands associated with transcriptional start sites and CpG methylation is associated with inhibition of transcription [90]. The human NIS gene has three CpG-rich regions. One region is located in the promoter, extending upstream for about 100 base pairs from the transcription start site. Two additional CpG-rich sequences are present downstream from this region with one of them extending to the first intron and the other to the coding region within the first exon [86]. Previous studies have failed to demonstrate specific patterns of DNA methylation that may be associated with failure of NIS transcription [91, 92]. However, a study that evaluated the effects of 5-azacytidine (a demethylating agent) combined with sodium butyrate (HDAC inhibitor) reported restoration of hNIS mRNA levels in four and iodide transport in two of the seven thyroid cancer cell lines investigated. Furthermore, analysis of the methylation patterns in these cell lines revealed that successful restoration of hNIS transcription was associated with demethylation of hNIS DNA in the untranslated region within the first exon [91].

Intriguingly, NIS expression is inhibited by Tg, which seems to act as negative regulator of the expression of NIS and other thyroid-specific genes (including Tg itself, TPO and TSH receptor). This suppressor effect of Tg is dependent on its ability to bind to the apical surface of thyrocytes [93]. NIS expression is also inhibited in the presence of oestrogens that also have progoitrogenic effects secondary to their combined effects of increased cell growth and reduced NIS expression [94].

## EXTRATHYROIDAL NIS

The first comprehensive review of the important iodide concentrating mechanisms outside the thyroid gland was performed by Brown-Grant in 1961 [95], but there has been a considerable shift in scientific opinion since then. The non-thyroidal tissues that actively accumulate iodide include the salivary glands, gastric mucosa, lactating mammary gland, choroid plexus and ciliary body of the eye. Iodide transport in most extra-thyroidal tissues is inhibited by perchlorate/thiocyanate [1]. Moreover, there are several reports of patients suffering hereditary simultaneous absence of iodide transport in the thyroid, salivary glands and gastric mucosa, suggesting that these effects are mediated through a common gene [95–97].

Isolation of rNIS cDNA and the generation of anti-NIS Ab facilitated characterization of NIS expression in extra-thyroidal tissues [98–100]. Subsequent analyses have confirmed beyond doubt that iodide transport in most extra-thyroidal tissues is NIS-mediated in a manner similar to that observed in the normal thyroid gland [101]. However, there are certain important differences in iodide metabolism and the regulation of NIS expression in extra-thyroidal tissues, when compared to normal thyroid gland. First, NIS expression in extra-thyroidal tissues is independent of TSH stimulation and is modulated by other tissue-specific hormonal regulators (see below). Second, extra-thyroidal tissues are devoid of an efficient iodide organification mechanism, secondary to the lack of an appropriate colloid protein (i.e. Tg) and corresponding iodide coupling (i.e. TPO) enzyme system. In this respect, the situation may be compared to that observed in PTU-treated thyroid tissue. However, as non-thyroidal tissues expressing NIS are not the site of any iodide-based

hormone synthesis, the lack of iodide organification is not associated with any physiological consequences. An exception to this general principle may exist in the lactating mammary gland where lactoperoxidase is capable of mediating iodination of milk proteins, such as casein [102].

NIS expression is differentially regulated in extra-thyroidal tissues compared to the thyroid gland and this is associated with important post-translational modifications leading to modest structural variations in the nature of the mature NIS polypeptides generated. Previous immunoreactivity experiments have demonstrated that mammary NIS matures into a 75 kDa polypeptide compared to the larger polypeptide isolated from the thyroid gland. This has been attributed to differences in post-translational modification (glycosylation) [103]. Iodide transport in the mammary gland occurs during late pregnancy and lactation. Studies investigating the possible regulatory mechanisms have shown that prolactin stimulates iodide transport in mammary gland explants [104]. Consistent with these findings is the observation that NIS is absent in mammary glands from nubile rats and that NIS expression is increasingly detectable toward the end of gestation and in lactating mammary gland. Furthermore, NIS expression is regulated in a reversible manner by suckling during lactation [103]. Further *in vivo* studies in ovariectomized mice have shown that the combination of estradiol, oxytocin and prolactin is associated with the highest level of NIS expression [1].

The physiological role of NIS expression and function in salivary glands and gastric and rectal mucosa is poorly defined. In the salivary glands, NIS protein has been detected in the basolateral membrane of all ductal epithelial cells [103, 105, 106]. In a similar manner, NIS protein is present in the basolateral membrane of mucin-secreting epithelial cells [103, 106]. Gastric NIS matures into an approximately 100 kDa gastric polypeptide and, again, the differences in electrophoretic mobility have been attributed to differences in glycosylation status [103].

Although NIS is expressed in the lactating mammary gland in normal circumstances, NIS expression has been observed in a large proportion of breast adenocarcinomas. Using *in vivo* scintigraphic imaging of experimental mammary adenocarcinomas in non-gestational and non-lactating female transgenic mice carrying either an activated ras oncogene or overexpressing the HER2/neu oncogene, Tazebay *et al.* (2000) demonstrated pronounced, active and targeted expression of NIS. Furthermore, functional NIS activity was inhibited by perchlorate [103]. Immunohistochemistry of breast cancer specimens showed that 87% of 23 human invasive breast cancers and 83% of 6 ductal carcinomas *in situ* expressed NIS. More importantly, only 23% of 13 extratumoural samples from the vicinity of the tumours and none of the eight normal samples expressed NIS. Both plasma membrane and intracellular pattern of NIS staining was observed in malignant breast tissue, in contrast with the distinct basolateral plasma membrane staining of lactating mammary gland tissues [103]. The same group has subsequently developed a flow cytometry-based assay for the early detection of mammary NIS expression in fine needle aspiration specimens [1].

Wapnir *et al.* (2003) studied NIS protein expression in 371 human breast samples and found NIS positivity in 76% of invasive breast carcinomas, 88% of ductal carcinomas *in situ* and 80% of fibroadenomas. In contrast, the majority of normal breast samples (87%), excluding gestational/ lactational changes, were negative [107]. The potential diagnostic and therapeutic value of mammary gland NIS expression in human breast cancer becomes apparent when comparing the proportion of NIS-expressing tumours (>75%) to those expressing the HER2/neu oncoprotein (33%). However, the proportion of breast tumours with functional NIS expression may be much lower, as shown by a study of  $^{99m}\text{TcO}_4^-$  scintigraphy that demonstrated positive uptake in only 4 out of 25 patients with breast

tumours [108]. In another study, 27 women were scanned with  $^{99m}\text{Tc}$  or  $^{123}\text{I}$  to assess NIS activity in their breast carcinoma metastases. NIS expression was evaluated in index and/or metastatic tumour samples by immunohistochemistry. Iodide uptake was noted in only 25% of NIS-expressing tumours (2 out of 8) [109]. It has been recently suggested that the PI3-K pathway is likely to play a major role in the discordance between NIS expression and iodide uptake in breast cancer patients [110].

### Pharmacological Modulation of Extrathyroidal NIS Expression

As a large proportion of extra-tumoural specimens did not express NIS in the above studies, the possible use of radioiodide ( $^{131}\text{I}$ ) therapy in these circumstances should be associated with a tumour-specific cytotoxic effect combined with an improvement in therapeutic index. This has prompted several investigators to look at different ways of enhancing functional NIS expression in breast cancer. The non-selective ATRA and also the isoform-selective RAR agonists have been investigated in breast cancer with the aim of inducing endogenous and functional NIS expression. Retinoids have a robust effect in inducing functional NIS in MCF-7 cells [111–113]. ATRA at a concentration of 1  $\mu\text{M}$  has been shown to increase iodide uptake, to 10-fold above baseline, in 3 different MCF-7 sub-clones. In contrast, the ER-negative breast cancer cell line MDA-MB 231 showed neither NIS expression nor iodide uptake, even after ATRA treatment [114]. Significant inductions of iodide uptake and NIS mRNA have been observed with isomers of ATRA, 9-*cis* RA and 13-*cis* RA [111–113]. ATRA and 9-*cis* RA stimulate formation of heterodimers of RAR and RXR and the RAR–RXR complex binds to its *cis*-element (retinoic acid response element (RARE)) on a target gene to stimulate or suppress transcription. 13-*cis* RA has a low affinity for RARs and RXRs [115] and stimulates RARs after isomerization to ATRA or 9-*cis* RA [116]. Differential regulation of gene expression by activation of each RAR isomer has been reported. The RAR $\beta/\gamma$  agonist AGN190168 is a more potent inducer of functional NIS expression than AGN195183 (RAR $\alpha$  agonist), AGN194433 (RAR $\gamma$  agonist) or AGN194204 (pan-RXR ligand), suggesting a central role of RAR $\beta$  in NIS induction by retinoids [112]. ATRA induces NIS gene expression partially at the transcriptional level [45]. The consensus sequence of RARE contains two of the core motifs, 5'-PuG[G/T][T/A]CA-3', directly repeating with a spacer of two or five bases (DR-2 or DR-5). Sequence inspection of the human NIS gene has revealed two consensus DR-2 elements (AGGTCAGGAGTTCA) in the first intron. However, it is not the putative DR-2 elements, but the DR-5 elements that are involved in the response to ATRA stimulation in MCF-7 cells [117]. Recently, the cardiac homeobox transcription factor, Nkx-2.5, was also shown to be induced by RA in MCF-7 cells and involved in the RA induction of NIS, using the rat proximal promoter in MCF-7 cells [118]. *In vivo* studies with MCF-7 xenograft tumours in immunodeficient mice have demonstrated that induction of iodide uptake in the tumour by systemic ATRA treatment increases iodine concentration up to 15-fold above background [114]. This was associated with a modest increase in the level of intracellular NIS expression, but ATRA stimulation did not induce NIS trafficking to the membrane. Furthermore, the iodide uptake and expression reduced within 2 days of the level of maximum induction. Nevertheless, the present evidence indicates that the effect of ATRA on NIS induction in breast cancer is fairly robust. More interestingly, there are no reports of retinoid-induced NIS induction in other NIS-expressing organs (thyroid, stomach, normal mammary gland), suggesting a degree of tumour-specificity with attendant important therapeutic implications [119].

Dexamethasone has been shown to significantly increase RA-induced iodide uptake, partially by stabilizing NIS mRNA [112]. This has been reported to reduce the median effective concentration of ATRA for the induction of iodide uptake. In a recent study reported by Unterholzner *et al.* (2007), incubation of MCF-7 cells with dexamethasone in the presence of ATRA was associated with an 11-fold increase in NIS mRNA levels in a

dose-dependent manner. In a similar manner, a 16-fold increase in NIS protein levels and upto 3- to 4-fold increase in the level of iodide uptake was observed. Furthermore, this was associated with modest reduction in the level of iodide efflux. Use of therapeutic radioisotope ( $^{131}\text{I}$ ) in these circumstances was associated with an increased cytotoxic effect. Selective cytotoxicity of  $^{131}\text{I}$  was significantly increased from approximately 17% in MCF-7 cells treated with ATRA alone to 80% in MCF-7 cells treated with Dex in the presence of ATRA [120]. Combined treatment with ATRA/dexamethasone *in vivo* was associated with significant  $^{123}\text{I}$  accumulation in MCF-7 xenografts that, by *ex vivo* gamma counting, revealed a 3.3-fold increase in iodide accumulation as compared to control tumours treated with ATRA alone. NIS mRNA and protein expression were detectable in ATRA/Dex treated MCF-7 tumours by RT-PCR and immunohistochemistry, respectively [121]. These encouraging results have set the stage for further studies aiming to exploit the potential reporter and therapeutic functions of NIS in managing breast cancer.

## GENETICALLY TARGETED RADIOISOTOPE THERAPY USING NIS

Radioisotopes are unstable forms of an element that have an imbalance in the relative numbers of protons and neutrons. As a consequence, they decay to emit particulate and/or electromagnetic radiation, both of which may be useful in treating tumours. Radioisotopes are used therapeutically as either sealed or unsealed sources. Sealed sources are used to deliver brachytherapy - whereby a radioisotope contained within an inert casing is placed on the surface of a tumour (mould brachytherapy) or within its substance (interstitial brachytherapy) or within the lumen of a hollow viscus (intraluminal brachytherapy) or cavity (intracavitary brachytherapy). At the end of the treatment period when the prescribed dose has been delivered, the radioactive sources are removed from the patient who remains uncontaminated by the radioisotope. In contrast, unsealed sources are radioisotopes which are not confined within a container and that come into contact with the patient through direct ingestion or injection. They are selectively absorbed in target tissues and deliver radiation dose through emission of decay particles (usually  $\alpha$  or  $\beta$  particles), although they also deliver dose to any non-target tissues in which they localise. The use of unsealed radioisotopes as a means of delivering radiation dose to tumours is well established in a relatively small number of clinical scenarios, including thyroid cancers ( $^{131}\text{I}$ ,  $^{111}\text{In}$ -octreotide) [2, 122], prostate cancer ( $^{89}\text{Sr}$ ,  $^{223}\text{Ra}$ ) [123, 124], neuroblastoma/phaeochromocytoma ( $^{131}\text{I}$ -meta-iodobenzyl-guanidine) [125] and lymphomas ( $^{90}\text{Y}$ -labelled anti-CD20 monoclonal antibody) [126].

The rapid developments in understanding the biology of NIS that have been detailed above have raised the possibility of using NIS-targeted therapeutic radioisotopes to treat non-thyroid cancers. This may involve treating tumours that endogenously express NIS (eg breast cancer) or those that have been induced to express NIS through exogenous methods of gene transfer. When cytoreductive NIS gene therapy was first proposed, it was greeted with considerable scepticism, as it was felt that the lack of iodide organification in non-thyroidal tissues would limit iodide retention and defeat the therapeutic purpose. However, there is no hard evidence to support the view that iodide organification is absolutely essential for radioiodide therapy. Moreover, thyroid cancer metastases often display a disrupted follicular architecture and lack Tg expression, both of which are associated with ineffective iodide organification, and yet radioiodide therapy against these metastases is effective [1]. In addition, therapeutic studies by Spitzweg and colleagues, in prostate cancer cell lines following exogenous gene transfer have conclusively demonstrated that radioiodide treatment can be effective, even in the absence of iodide organification [127–129].

Targeted radioisotope therapy is associated with at least two types of bystander effect. The first is decay particle cross-fire of neighbouring untransduced cells by adjacent transduced cells that have accumulated radioisotope. The second effect is due to conversion of the physical insult of irradiation into chemical signals by the exposed cell, perhaps in the form of reactive oxygen species (ROS) or cytokines. This latter so-called radiation-induced biological bystander effect (RIBBE) may induce chromosomal aberrations, genomic instability and cell death in untransduced, unirradiated cells. There is considerable evidence that RIBBE occurs in tissues and may contribute to death of cells not directly in the radiation track [130, 131].

### Preclinical Studies of NIS Gene Transfer by Replication-Defective Viruses

NIS gene therapy has undergone extensive pre-clinical evaluation. Fig. (3) is a schematic illustration of the important principles of vector (adenoviral)-mediated NIS radioiodide therapy in an experimental tumour model. Shimura *et al.* (1997) first successfully transfected rNIS cDNA by electroporation into malignant transformed rat thyroid cells (FRTL-Tc) with restoration of iodide transport activity. FRTL-Tc cells stably expressing rNIS accumulated  $^{125}\text{I}$  60fold *in vitro* and xenotransplants in Fischer 344 rats derived from the same stably transfected cell line trapped up to 27.3% of the total  $^{125}\text{I}$  dose with an effective half-life of approximately 6 hours. A therapeutic dose of 1 mCi  $^{131}\text{I}$  did not, however, cause statistically significant tumour volume reduction [127].

Since then several studies have demonstrated the feasibility of inducing functional NIS expression in extrathyroidal tumours [133]. Cho *et al.* (2000) evaluated the expression and activity of hNIS in cultured human glioma cells following adenovirus-mediated gene delivery *in vitro* and *in vivo*. Delivery of exogenous hNIS *in vitro* resulted in more than a 120-fold increase in iodide uptake in U1240 cells infected with recombinant adenovirus expressing hNIS regulated by the CMV promoter. Intratumoural injection of Ad-CMV-hNIS into subcutaneous xenografts of U251 human gliomas resulted in a 25-fold increase in  $^{125}\text{I}$  accumulation compared to the spleen or saline-injected tumours [134]. Mandell *et al.* (1999) demonstrated *in vitro* and *in vivo* iodide accumulation in melanoma, liver, colon and ovarian carcinoma cells after retrovirus-mediated transfection with rNIS. NIS-transduced melanoma xenografts accumulated significantly more  $^{123}\text{I}$  (6.9-fold increase) than non-transduced tumours [135]. Similarly Boland *et al.* (2000) used adenoviral-mediated NIS (CMV promoter) gene delivery to demonstrate functional levels of NIS expression in several tumour cell lines (cervix, prostate, breast, lung and colon carcinoma cells). Fold increases in iodide uptake of 125–225 times were observed *in vitro*. Eleven per cent of the total I dose could be recovered per gram of adenovirus-infected tumour tissue (breast and cervix xenografts). Although an *in vitro* cytotoxic effect was observed, the study failed to demonstrate an *in vivo* therapeutic effect. However, this was possibly secondary to the low intraperitoneal doses of  $^{131}\text{I}$  (90  $\mu\text{Ci}$ ) used in the study [136]. Nakamoto *et al.* (2000) stably transfected the human breast cancer cell line (MCF-7) with the rNIS gene using electroporation and demonstrated a 44-fold increase in radioiodide uptake *in vitro* and reasonable levels of retention (16.7%) of the total  $^{125}\text{I}$  dose administered *in vivo* [137]. Spitzweg *et al.* (1999) first demonstrated tissue-specific expression of hNIS cDNA in androgen-sensitive human prostate adenocarcinoma (LNCaP) following transfection with a eukaryotic expression vector in which the full-length hNIS cDNA was coupled to a prostate-specific antigen (PSA) promoter. Prostate cells transfected with PSA-NIS showed perchlorate-sensitive, androgen-dependent iodide uptake. In contrast, cells transfected with the PSA-NIS and deprived of androgen or cells transfected with control vectors failed to retain iodide [127]. The same group were also the first to demonstrate the feasibility and effectiveness of NIS-mediated cytotoxicity *in vivo* and, in the process, allayed concerns that NIS-mediated therapy was unlikely to succeed due to lack of iodide-organification in non-

thyroid tumours. They employed LNCaP cell lines stably transfected with hNIS-cDNA (NP-1) under the control of a PSA promoter (NP-1 cells) and showed perchlorate-sensitive, androgen-dependent iodide uptake *in vitro* that resulted in selective killing of these cells by radioiodide ( $^{131}\text{I}$ ) in an *in vitro* clonogenic assay. Xenografts were established in athymic nude mice and imaged using a gamma camera after intraperitoneal injection of 500  $\mu\text{Ci}$  of  $^{123}\text{I}$ . In contrast to the NIS-negative control tumours (P-1) that showed no *in vivo* iodide uptake, NP-1 tumours accumulated 25–30% of the total  $^{123}\text{I}$  administered with a biological half-life of 45 hours. In addition, NIS protein expression in LNCaP xenografts was confirmed by Western analysis and immunohistochemistry. More interestingly, a single therapeutic dose of 3 mCi  $^{131}\text{I}$  yielded a dramatic therapeutic response in NIS-transfected LNCaP xenografts, with an average volume reduction of more than 90% and complete tumour regression in 60% of tumours [128]. The same group subsequently employed a replication-deficient human adenovirus incorporating the human NIS gene driven by the CMV promoter (Ad5-CMV-NIS) for *in vivo* NIS gene transfer into LNCaP tumours. Following intraperitoneal injection of a single therapeutic dose of 3 mCi  $^{131}\text{I}$  4 days after adenovirus-mediated intratumoural NIS gene delivery, LNCaP xenografts showed a clear therapeutic response with an average volume reduction of more than 80% [129].

Cho *et al.* (2002) reported on results from a study aimed at investigating the therapeutic and reporter applications of NIS gene transfer in an animal model of intracerebral gliomas. F98 glioma cells were transduced with a recombinant retrovirus containing hNIS (L-hNIS-SN) driven by the Moloney murine leukemia virus LTR promoter. Radioiodide uptake in hNIS-transduced F98 rat glioma cells (F98/hNIS) was 40-fold higher than parental F98 cells and was inhibited by perchlorate. Rat glioma cells (F98/LXCN) transduced with empty vector did not show enhanced iodide uptake. hNIS expression was demonstrated by Western analysis in transduced cells (mainly in the 90 kDa glycosylated form). Using  $\text{TcO}_4$  scintigraphy, it was possible to visualise intracerebral gliomas (F98/hNIS) at eleven days after tumour implantation, when the tumour measured 4.5×3.8 mm.  $^{123}\text{I}$  scintigraphy confirmed radioiodide retention in F98/hNIS gliomas. Rats were injected with 250  $\mu\text{Ci}$   $^{123}\text{I}$  via the tail vein and gamma camera images were acquired at different time points after injection. Radioiodide uptake was evident in F98/hNIS gliomas up to 24 hrs after injection. However, I uptake was barely detectable in F98/hNIS gliomas at 37 hrs after injection. Based on the time-activity curve, the biological half-life of  $^{123}\text{I}$  in F98/hNIS gliomas was estimated to be 10 hrs, compared to the biological half-life of more than 20 hrs in the normal thyroid gland. Importantly, the authors demonstrated that intrinsic thyroidal NIS expression and iodide uptake could be markedly inhibited by thyroxine (T4) supplementation of the diet. In the therapeutic model, animals received three intraperitoneal injections (4 mCi each) of  $^{131}\text{I}$  on days 12, 14 and 16 after tumour implantation. The average survival time of the rats with F98/hNIS tumours with  $^{131}\text{I}$  treatment was prolonged compared with that of rats with F98/LXSn tumours with  $^{131}\text{I}$  treatment (2 weeks longer,  $P < 0.01$ ). However, no significant difference in the size of the tumours was observed within the two groups at the time of death. Rather interestingly, the rats bearing F98/hNIS tumours not treated with radioiodide had a survival time longer than rats bearing parental F98 tumours ( $39.0 \pm 4.1$  days vs  $30.4 \pm 3.2$  days). Tumour inhibitory properties of the normal sodium/iodide retained by the hNIS transduced cells and the host immune response to hNIS cells were some of the hypotheses put forward by the investigators to explain the above phenomenon [138].

Kakinuma *et al.* (2003), reported on a study that evaluated adenoviral-mediated NIS expression regulated by the tissue-specific probasin promoter in prostate and various other tumour cell lines. Following infection with a replication-deficient adenoviral vector expressing NIS cDNA from a composite probasin promoter (ARR(2)PB), androgen-dependent and perchlorate-sensitive iodide uptake was demonstrated in LNCaP cells that was 3.2-fold higher compared to the Ad-CMV/hNIS vector. Furthermore, iodide uptake in a

panel of non-prostate tumour cell lines infected with Ad-ARR(2)PB/hNIS was significantly lower, indicating the tissue specificity of this construct [139].

Sieger *et al.* (2003), investigated radioiodide uptake in a hepatoma cell line *in vitro* and *in vivo* after transfer of the sodium iodide symporter (hNIS) gene under the control of a tumour-specific regulatory element, the promoter of the glucose transporter 1 (GT1) gene (GTI-1.3). NIS-expressing stable cell lines (rat hepatoma (MH3924A)) demonstrated perchlorate-sensitive increased iodide uptake (30-fold increase *in vitro* and 22-fold increase *in vivo*) compared to the wild-type cell line. Similarly, the mean radiation dose delivered to MH3924A xenografts was 10-fold higher (85 mGy compared with 830 mGy) following administration of 18.5 MBq of  $^{131}\text{I}$  [140]. The same group performed a further study on iodide kinetics in NIS-expressing rat prostate adenocarcinoma cell lines (Dunning R3327 subline AT1). NIS-expressing stable cell lines were generated following trans-fection with a retroviral vector expressing NIS regulated by the tumour-specific regulatory element, the elongation factor 1 $\alpha$  (EF1- $\alpha$ ) promoter. NIS-expressing cells showed increased iodide uptake, but this was associated with rapid efflux. *In vitro*, rapid efflux of the radioactivity (80%) was observed during the first 20 minutes after replacement of the medium. Similarly, the hNIS-expressing xenografts had lost upto 91% of the initial activity at 24 hours. The authors subsequently demonstrated flattening of the *in vivo* dose-response curve with increasing  $^{131}\text{I}$  concentration that was attributed to the rapid iodide efflux. For example, 1200 MBq/m $^2$  of  $^{131}\text{I}$  was associated with a mean tumour dose (MTD) of 3+/-0.5 Gy (wild-type tumour 0.15+/-0.1 Gy) and 2400 MBq/m $^2$  with MTD of 3.1+/-0.9 Gy (wild-type tumour 0.26+/-0.02 Gy) [141]. Further to this, Faivre *et al.* (2004) reported on an *in vivo* kinetic study of NIS-related iodine uptake in an aggressive model of hepatocarcinoma induced by diethylnitrosamine in immunocompetent Wistar rats. An adenoviral vector expressing rNIS regulated by the CMV promoter (Ad-CMV-NIS) was injected into the portal vein of 5 healthy and 25 hepatocarcinoma-bearing rats. This was associated with marked (from 20 to 30% of the injected dose) and sustained (>11 days) iodide uptake that contrasted with the rapid iodide efflux observed *in vitro*. Prolonged retention of iodide observed *in vivo* was not attributed to an active retention mechanism, but to permanent recycling of the effluent radioiodine via the high hepatic blood flow. Ra-dioiodine therapy in these circumstances was associated with strong inhibition of tumour growth, complete regression of small nodules and prolonged survival of hepatocarcinoma-bearing rats [142].

Gaut *et al.* (2004) reported on a study of NIS-mediated radioiodide therapy in a head and neck cancer model. Using a NIS-expressing AV vector regulated by the CMV promoter, they demonstrated a perchlorate-sensitive increase (upto 25-fold) in iodide uptake in transduced cell lines (FaDu, SCC-1 and SCC-5). Treatment with  $^{131}\text{I}$  was associated with a dose-dependent increase in cytotoxicity with an observed 80% reduction in cell survival on an *in vitro* clonogenic assay. Similarly, an *in vivo* therapeutic dose of  $^{131}\text{I}$  (1 mCi) was associated with a delay in the growth of NIS-transduced tumours in athymic nude mice. Moreover, when radioiodide was administered to mice with established xenografts of stably transfected NIS-expressing FaDu cells, almost complete tumour regression was observed [143].

Schipper *et al.* (2005) reported on the results of NIS-mediated radioiodide therapy in a neuroendocrine cancer model. The study was performed in Bon1 and QGP pancreatic neuroendocrine tumour cells. NIS gene delivery was mediated by plasmids expressing hNIS cDNA regulated by the CMV promoter or by the tissue-specific chromogranin A promoter. Chromogranin A is produced by 80–100% of neuroendocrine tumours and serves as a reliable biochemical marker. A 20-fold increase in iodide uptake was observed following transfection with the plasmid expressing NIS regulated by the chromogranin A promoter. This contrasted with an up to 50-fold increase in iodide uptake observed following CMV

promoter-driven NIS expression. Maximal uptake was reached within 15 minutes in QGP cells and 30 minutes in Bon1 cells, with an effective half-life of 5 minutes and 30 minutes, respectively. However, no evidence of organification was detected by high-performance liquid chromatography and gel-filtration chromatography to account for the longer half-life of iodide in the Bon1 cells.  $^{131}\text{I}$  was highly effective in preventing the formation of QGP and Bon1 cell clones in the *in vitro* clonogenic assay. Clonogenic survival was reduced in the NIS-expressing QGP and Bon1 cells by 99.8 and 98.8%, respectively, after incubation with 100  $\mu\text{Ci/ml}$  of  $^{131}\text{I}$  [144].

Cengic *et al.* (2005) assessed the feasibility of radioiodide therapy of medullary thyroid cancer (MTC) after NIS gene transfer using the tissue-specific calcitonin promoter to target hNIS gene expression to MTC cells. MTC cells were stably transfected with an expression vector, in which hNIS cDNA was coupled to the calcitonin promoter. hNIS-transfected cells showed a perchlorate-sensitive, 12-fold increase in iodide uptake. Furthermore, this was associated with *in vitro* organification of 4% of the accumulated iodide, resulting in a significant decrease in iodide efflux. In an *in vitro* clonogenic assay, 84% of NIS-transfected cells were killed by exposure to  $^{131}\text{I}$  (0.8 mCi), compared to less than 1% of control cells [145]. Subsequently, the same group reported on results of a similar *in vitro* study performed in a colorectal cancer model. Colorectal (HCT116) cancer cells were stably transfected with hNIS cDNA coupled to the tissue-specific CEA promoter. The stably transfected HCT116 cells concentrated  $^{125}\text{I}$  about 10-fold *in vitro* without evidence of iodide organification. Furthermore, 95% of stably transfected HCT116 cells were killed by exposure to  $^{131}\text{I}$ , while only about 5% of NIS-negative control cells were killed [146].

Dwyer *et al.* (2005) reported on a study of *in vivo* NIS gene transfer followed by radioiodide imaging and treatment in a breast cancer model. They developed a replication-defective adenoviral construct expressing NIS under the control of the mucin-1 (MUC1) promoter (Ad5/MUC1/NIS) to target expression specifically to MUC1-positive breast cancer cells. MUC1 is a transmembrane glycoprotein that is overexpressed in many tumour types, including breast, pancreatic and ovarian cancers. A 58-fold increase in iodide uptake was observed in infected MUC1-positive T47D cells with no significant increase observed in MUC1-negative MDA-MB-231 cells or in cells infected with the control virus. Tumour xenografts were transduced with  $5 \times 10^8$  plaque-forming units (PFU) of recombinant Ad5-MUC1-NIS or control virus.  $^{123}\text{I}$  scintigraphy yielded clear images of the NIS-transduced tumour xenografts. Multiple images were acquired from 1 to 48 hours after iodide administration to determine the rate of iodide efflux from the tumours. The average tumour activities per gram (corrected for acquisition time, background and iodide decay) at 1, 3, 5 and 7 hours were 21%, 15%, 11% and 7%, respectively, and had decreased to <2% by the 24-hour time point. The biological half-life of the iodide in the tumour was calculated to be 5.8 hours. Administration of a therapeutic dose (3 mCi) of  $^{131}\text{I}$  resulted in an 83% reduction in the volume of NIS-transduced tumours, whereas control tumours continued to increase in size ( $P < 0.01$ ) [147]. Subsequently, the same group employed this strategy for *in vivo* radioiodide imaging and therapy of ovarian and pancreatic tumours. *In vitro* studies in pancreatic cancer cells revealed a 43-fold increase in iodide uptake in NIS-transduced cells compared with controls. Similarly, *in vivo* imaging revealed effective iodide uptake and retention at the site of NIS-transduced tumours, with optimal uptake (13% of injected dose) observed 5 hr after iodide administration. Intravenous injection of Ad5/CMV/NIS resulted in robust iodide uptake throughout mouse liver, whereas no uptake was detected in the liver of animals given Ad5/MUC1/NIS intravenously, thereby conclusively demonstrating the tissue-specificity of the MUC1 promoter. Therapeutic doses of  $^{131}\text{I}$  resulted in significant regression of NIS-transduced (Ad/MUC1/NIS) tumours, with a mean 50% reduction in volume within 10 weeks of therapy ( $p < 0.0001$ ) [148]. Transduction of ovarian tumour cells with the Ad/MUC1/NIS vector was associated with a 5-fold increase in iodide uptake *in*

*vitro*, compared to a 12-fold increase in iodide uptake with Ad/CMV/NIS. *In vivo*  $^{123}\text{I}$  scintigraphy revealed clear tumour visualisation following transduction with the Ad/CMV/NIS vector. In contrast, the tumour visualisation following transduction with the Ad/MUC1/NIS vector was less intense. These results were in keeping with the therapeutic studies that showed a significant reduction (53%) in tumour volume ( $p < 0.0001$ ) with a therapeutic dose of  $^{131}\text{I}$  following transduction with the Ad/CMV/NIS vector. However,  $^{131}\text{I}$  administration following transduction with the Ad/MUC1/NIS vector was not associated with tumour regression, although at 8 weeks after therapy the mean relative tumour volume in the NIS-transduced group was significantly lower compared to the non-transduced controls, indicating slowing in the rate of tumour progression (166 versus 332%,  $p < 0.05$ ) [149].

In keeping with the above observation, a group from China recently published results from another study aimed at optimising the above strategy for the treatment of pancreatic cancer where NIS expression was driven by the tumour-specific MUC1 promoter. A 23- and 15.5-fold increase in iodide uptake was observed in Ad/MUC1/NIS-infected MUC1-positive Capan-2 (pancreas) and SW1990 (pancreas) cells with no significant increase observed in MUC1-negative Hela (cervical) cells or in cells infected with the control virus. Capan-2 xenografts were established in nude mice and transduced with  $5 \times 10^8$  PFU of Ad-MUC1-NIS vector. Subsequent intraperitoneal administration of 0.5 mCi of  $^{123}\text{I}$  allowed visualisation of tumours using conventional gamma camera imaging. The rate of iodide efflux was determined using serial image acquisition. The average tumour activities per gram at 1, 3, 5 and 7 hrs were 10.8, 12, 9.9 and 7%, respectively, and had decreased to 3% by the 24 hour time point with an effective biological half-life of 10.5 hrs. Following a therapeutic dose of  $^{131}\text{I}$  (3 mCi), Ad/MUC1/hNIS-infected tumours regressed to  $76 \pm 15\%$  of their original volume ( $p < 0.05$ ) within 7 weeks of therapy [150].

Spitzweg *et al.* (2007) reported on a study of a novel therapeutic strategy aimed at assessing the effects of tissue specific NIS expression using the CEA promoter in a model of MTC. Using  $^{123}\text{I}$  scintigraphy, they demonstrated that MTC cell xenografts injected with the Ad5-CEA-NIS vector ( $5 \times 10^8$  PFU) accumulated  $7.5 \pm 1.2\%$  ID/g (injected dose per gram) of iodide with an average biological half-life of  $6.1 \pm 0.8$  hrs. Administration of a therapeutic dose (3 mCi) of  $^{131}\text{I}$  resulted in a significant reduction of tumour growth associated with significantly lower calcitonin serum levels in treated mice as well as improved survival [151]. More recently, the same group has published on another study in which NIS expression was driven by the tumour specific promoter (alpha-fetoprotein (AFP)) in a hepatocellular carcinoma model. Murine Hepa 1-6 and human HepG2 hepatoma cell lines were stably transfected with NIS cDNA under the control of the tumour-specific AFP promoter. Following exposure to  $^{131}\text{I}$ , more than two-thirds of NIS-transfected cells were killed compared to less than 5% of the control population. NIS-transfected HepG2 xenografts accumulated 15% of the total  $^{123}\text{I}$  administered per gram of tumour with a biological half-life of 8.38 hr, leading to an estimated tumour absorbed dose of 171 mGy  $\text{MBq}^{-1}$   $^{131}\text{I}$ . Administration of 1.5 mCi of  $^{131}\text{I}$  was associated with significant inhibition of tumour growth *in vivo* [152].

In addition to the above *in vivo* studies primarily performed in rodents, a preclinical dosimetric study of NIS-mediated radioisotope therapy has been performed in adult male beagle dogs. This was a safety and feasibility study that was carried out in preparation for a Phase I clinical trial to be performed in patients with locally recurrent prostate cancer. In this study, animals received direct intraprostatic injections of  $1 \times 10^{12}$  viral particles of NIS-expressing AV vectors regulated by the CMV promoter. This was followed by intravenous injection of 3 mCi  $^{123}\text{I}$  and serial image acquisition using SPECT/CT. This revealed clear images of the prostate in all dogs that were injected with Ad5/CMV/NIS and none in the group injected with the control virus. The level of uptake in each organ was expressed as a

percentage of the total activity and used to estimate the dose of radioiodide delivered to each organ. The average absorbed dose to the prostate was estimated to be  $23 \pm 42$  cGy/1 mCi  $^{131}\text{I}$ . This indicated that an 85 mCi dose of  $^{131}\text{I}$  would be sufficient to obtain a target dose of 2000 cGy to the prostate. Following a therapeutic dose of  $^{131}\text{I}$  ( $116 \text{ mCi/m}^2$ ), preceded by T3 supplementation ( $0.7 \mu\text{g/kg}$ ) for 8 days, the estimated mean doses delivered to the prostate, thyroid, stomach and liver were  $1245.1 \pm 280.9$ ,  $12.0 \pm 0.99$ ,  $23.2 \pm 2.00$  and  $0.89 \pm 0.63$  cGy/mCi of  $^{131}\text{I}$ . No major toxicities or changes in blood biochemistries were noted. This was the first study of its kind to assess the reporter and possible therapeutic functions of NIS-mediated radioisotope therapy in large animals that involved administration of therapeutic doses of I similar to those used in the clinical setting [153].

In summary, the above studies have conclusively demonstrated the feasibility of using NIS-mediated radioisotope therapy in a wide variety of tumour models. These studies have employed various methods of gene delivery, ranging from simple plasmid-mediated delivery regulated by the constitutive CMV promoter to more complicated genetically engineered viral vectors incorporating NIS driven by tumour- (GT-1, EF1- $\alpha$ , AFP), or tissue-specific promoters (PSA, probasin, CEA, MUC1). Key-points of the design and outcome from the above studies have been summarised in Table 1.

### Preclinical Studies of NIS Gene Transfer by Replication-Competent Viruses

Until recently, much of the focus of virus-mediated NIS delivery was predicated on the notion of using viruses purely as vehicles to deliver the therapeutic genes. However, within the last 5 years there has been a significant shift in attitudes in favour of the use of replication-competent or oncolytic virus vectors which has principally been driven by recognition of their greater potency (due to their intrinsic cytotoxicity and their ability to self-amplify and, thus, increase the level of transgene expression) and their impressive safety record.

A number of NIS-expressing oncolytic agents have been assessed. We recently reported *in vivo* SPECT imaging of the time-course of gene expression from two oncolytic adenoviruses expressing NIS in tumor-bearing mice [154]. In these viruses, the hNIS cDNA was positioned in the E3 region either in a wild-type adenovirus type 5 (AdIP1) or one in which a promoter from the human telomerase gene (RNA component) was driving E1 expression (AdAM6). Viruses showed functional hNIS expression and replication *in vitro* and the kinetics of spread of the two viruses in tumour xenografts were visualized *in vivo* using a small animal nano-SPECT/CT camera. The time required to reach maximal spread was 48 h for AdIP1 and 72 h for AdAM6 suggesting that genetic engineering of adenoviruses can affect the kinetics of their dissemination in tumours. More recently, we have shown that a Wnt-targeted oncolytic adenovirus expressing NIS can mediate a specific oncolytic effect that is augmented by the additional delivery of  $^{131}\text{I}$  [155]. In addition, SPECT imaging studies allowed careful evaluation of the optimal therapeutic schedule for virus administration and subsequent radioisotope delivery. Thus, a single radioisotope dose delivered 48 hours after virus administration resulted in very significant anti-tumour efficacy.

A recombinant NIS-expressing Edmonston strain measles virus (MV-NIS) has also been shown to have significant potential both as an *in vivo* imaging tool and as a therapeutic agent in combination with  $^{131}\text{I}$  [156]. An initial preclinical model of multiple myeloma demonstrated that MV-NIS was capable of mediating concentration of  $^{123}\text{I}$  such that intratumoral spread of the virus could be imaged by serial gamma camera imaging. In therapy experiments, when MV-NIS was combined with  $^{131}\text{I}$ , it was able to cause complete regressions of MM1 xenografts (which were resistant to virus therapy in the absence of radioisotope) [156]. Subsequent studies demonstrated that MV-NIS was active in mice

bearing intraperitoneal SKOV3 ovarian cancer [157] and subcutaneous BxPC-3 pancreatic cancer xenograft tumours [158, 159]. The promising nature of these studies has led to instigation of phase I clinical trials of MV-NIS in patients with a range of tumour types [160].

### Thyroid Gland Suppression as a Strategy During NIS Gene Therapy

Therapeutic radioiodide ( $^{131}\text{I}$ ) has been the most commonly employed radioisotope in the above studies. Radioiodide uptake in the thyroid gland is associated with organification and prolonged retention. In the long term, this will lead to radiation-induced hypothyroidism secondary to ablation of normal thyroid tissue. In addition, sequestration by the thyroid gland may reduce the uptake of radioiodide within the exogenously NIS-transduced tumour tissue, potentially compromising the therapeutic effect. For example, in the study by Spitzweg *et al.* (2000) the absorbed dose to the tumour was calculated to be 3.5 Gy after a 1 mCi dose of  $^{131}\text{I}$ . In comparison, the average absorbed dose to the thyroid was estimated at approximately 4.5 Gy/mCi  $^{131}\text{I}$ . In view of the above, it is important that some form of mechanistic strategy aimed at reducing iodide uptake within intrinsic thyroid tissue is incorporated within experimental protocols [128].

Cho *et al.* (2000), in one of the earlier studies on the effect of NIS-mediated  $^{131}\text{I}$  therapy in glioma xenografts (F98/hNIS), specifically looked at the effect of thyroxine (T4) supplementation on iodide uptake within the thyroid gland and NIS-transduced gliomas. As part of their study, rats were placed on 1 ppm thyroxine (T4)-supplemented diet for 1 week before the first day of  $^{131}\text{I}$  treatment. Rats fed on T4-supplemented diet did not show any uptake in the thyroid on subsequent  $^{99\text{m}}\text{TcO}_4^-$  scintigraphy. Furthermore, this correlated with a reduced level of NIS protein expression on western blot analysis [134]. Most subsequent studies have employed low-iodine diets combined with T4 supplementation (0.05–5 mg/l) for 1–2 weeks prior to radioiodide therapy [128, 150–153]. The effectiveness and feasibility of using this protocol can be gauged from the study by Wapnir *et al.* (2004) that was performed in patients with metastatic breast cancer [109]. In this study, T3 supplementation was effective in reducing thyroid iodide uptake to less than 2.8% at 24 hours. Iodide supplementation may also be employed to suppress iodide uptake within the thyroid gland. Potassium iodide (KI) (0.1–2%) administered for 24–48 hrs prior to treatment has been previously used to suppress thyroidal iodide uptake following administration of iodinated radiolabelled analogues. In a study by Dupertuis *et al.* (2001), KI (0.2 g/l) supplementation for upto 24 hours prior to administration of 3.7 MBq of iodinated 5-iodo-2'-deoxyuridine [ $^{125}\text{I}$ ]IdUrd significantly reduced iodide uptake in thyroid tissue [161]. There is, as yet, no evidence that iodide-induced suppression of NIS function and resulting iodide transport is prevalent outside the normal thyroid gland (*vide supra*). Therefore, KI supplementation appears to be a more pragmatic and convenient way of blocking iodide uptake within the thyroid gland in studies of NIS-mediated  $^{131}\text{I}$  therapy for the treatment of non-thyroid cancer.

### Optimisation of the Therapeutic Response to NIS

As discussed previously, one of the main caveats against the potential success of NIS gene therapy as a treatment for extra-thyroidal cancer has been the lack of an effective iodide retention mechanism. It has been shown previously that the effective biological half-life of  $^{131}\text{I}$  in these circumstances ranges from approximately 5–10 hours [147, 151, 152], which is far less than that observed within the normal thyroid gland.

Using a regression dosimetry model, O'Hare *et al.* (1998) estimated the effective half-life of  $^{131}\text{I}$  in the thyroid gland of a 30-year old male to be approximately 7.5 days [162]. The mean absorbed-dose by the thyroid gland after administration of  $^{131}\text{I}$  was estimated as

approximately  $0.70 \pm 0.09$  Gy MBq<sup>-1</sup> in a healthy non-iodine-deficient male. In the context of thyroid cancer patients, there is no consensus amongst physicians about the optimal prescribed activity and no routine measure of the dose absorbed by the lesions, in spite of the extensive use of the radioiodide in the treatment of thyroid cancer for the last 50 years. Physicians prescribe empirical activities to patients. In the field of radiation oncology, doses of external beam radiotherapy began from an empirical approach, but were modified as clinical and radiobiological data gave more insights in to the actual absorbed dose in tissues. Now the unit of radiotherapy is ‘absorbed dose’ measured in Gray (Gy).

However, dosimetry in radioisotope treatment has not developed in the same way because it is not simple and is dependent on many physiological factors. The empirical activity method, used for many decades, has been shown to be safe and effective. The most commonly used activity for ablation of a thyroid remnant is between 1.1 to 3.7 GBq. However, the success rates for ablation with this approach reach only up to 80% and patients with unsuccessful ablation have a higher chance of recurrence, anaplastic transformation and mortality [163]. The activity used for the treatment of residual or recurrent thyroid cancer also varies most commonly in the range of 5.5 to 11 GBq. Retrospective studies have shown that normal tissue toxicity with these activities is modest. Around 25% of the patients complain of mild to moderate xerostomia whilst myelosuppression is seen in a very low proportion of the patients usually following multiple treatments [164, 165].

Another problem with the empirical activity method is that the administered activity is not directly related to the absorbed dose. This is dependent on variables such as homogeneity of radioiodine uptake, pre-treatment TSH level, iodine deprivation of the body prior to the treatment, excretion rate of the radioiodine and biology of the tumour. ‘Whole body’ measurements of dose have been done in previous studies and can vary from 5% to 50% of the given dose at 48 hours. Most patients lie in the 10% to 25% range, thus emphasizing the importance of developing a more accurate dosimetric approach. In an attempt to make the prescription less empirical, Benua introduced a system to calculate and prescribe to absorbed dose in the whole blood compartment or bone marrow [166]. These doses correlated well with the toxicity profile. Their recommended safe maximum whole blood dose was 2 Gy with maximum body retention at 48 hours less than 4.4 GBq and, if lung metastases were present, less than 3 GBq. An advantage of this method is that potentially higher doses of the radioiodine can be delivered as long as these tolerance limits are respected. However, these measurements do not give any indication of the dose received by the tumour itself. Thus, the therapeutic impact of the dosimetry is not known.

Lesion-based dosimetry aims to measure the absorbed dose per lesion following delivery of the radioisotope [167]. This method aims to predict the activity needed in order to deliver a specific absorbed dose required to produce tumour cell kill in the target lesion. Patients are scanned serially following administration of a tracer radioisotope to establish patient specific biokinetics. Using these data, the radiation absorbed dose to thyroid cancer lesions can be estimated. The activity of radioiodine required to deliver a predicted absorbed dose can therefore theoretically be predicted from such a tracer study. Of course, there are limitations to such a method. The uptake of radioisotope into the tumour is assumed to be instantaneous and decay is assumed to be mono-exponential. When considering prediction of dose from the tracer study one assumes that the biokinetics of the tracer dose and the therapy dose are the same. If there is a difference the predicted dose to the tumour could be an over- or under-estimation.

Therefore, even in relatively well studied situations like ablation- or therapy-dose iodide treatment in thyroid cancer, there remain significant gaps in our understanding of the dosimetric issues. We do not have human studies of exogenous NIS gene transfer for direct

comparison. However, in the study by Dwyer *et al.* (2005) performed in adult male beagle dogs, the average absorbed-dose delivered to the prostate following intraprostatic injection of  $1 \times 10^{12}$  viral particles of Ad-CMV-NIS was estimated to be much lower at  $0.23 \pm 0.42$  Gy after an intravenous administration of 1 (37 MBq) mCi  $^{131}\text{I}$  [153]. The therapeutic effect observed in this situation is mediated by radioiodide-induced lethal and sublethal cellular DNA damage, which primarily depends on the area under the curve of the cumulative radioactivity within the cell. This, in turn, is governed by two important factors - the level of iodide uptake (function of cellular NIS expression) and the time spent by the iodide in the cell (function of iodide retention mechanisms). Therefore, further optimisation of the therapeutic effect may be achieved by modulation of the above two factors - enhancing the level of NIS expression and intracellular retention of iodide - with the aim of improving the area under the time-radioactivity curve and the resulting cytotoxic effect.

### Prolongation of Iodide Retention During NIS Gene Therapy

Previous studies have evaluated the effect of lithium on iodide-metabolism in NIS-expressing thyroid tissues and in NIS-deficient poorly differentiated thyroid cancer cell lines and extra-thyroidal cell lines following exogenous NIS transfer. Initial studies had shown that lithium diminished the release of  $^{131}\text{I}$  from papillary and follicular thyroid cancers, thus potentially increasing the absorbed radiation dose to the tumour [168–171]. This hypothesis was tested in a clinical study in patients with differentiated thyroid cancer, where lithium carbonate was administered prior to  $^{131}\text{I}$  scintigraphy. Lithium lengthened the biological half-life, with a mean increase of approximately 50% in tumours and 90% in thyroid remnants. Furthermore, lithium was relatively more effective in lesions with shorter biological half-lives of  $^{131}\text{I}$ . When the control biological half-life was less than 3 days, lithium prolonged the effective half-life in responding metastases by more than 50%. This was associated with an estimated  $2.29 \pm 0.58$ -fold increase in the absorbed radiation dose [170]. In a more recent study, the effect of lithium on iodide uptake was evaluated *in vitro* using the benign rat thyroid cell line FRTL-5 and the non-thyroid Madin–Darby canine kidney (MDCK) cell line stably transfected with human NIS. Interestingly, no effect of lithium carbonate on iodide uptake or efflux was observed in either of the cell lines. The investigators also carried out an evaluation of the effect of lithium on iodide uptake and tumour response *in vivo*. Twelve patients with metastatic DTC, who had received previous radioiodide therapy without lithium (control), were treated with 1200 mg lithium carbonate/day followed by 6000 MBq of  $^{131}\text{I}$ . Although, lithium increased the radioiodide uptake in seven patients, no beneficial effect of  $^{131}\text{I}$  with lithium was observed on the clinical course as assessed radiographically and by serum Tg measurements [171]. Similar results were observed in another study where lithium did not influence the iodide uptake of stably transfected NIS-expressing human anaplastic and medullary thyroid cancer-derived cell lines [172]. These conflicting data expose the potential limitations of using this pharmacological approach at optimising the level of intracellular iodide retention.

Huang *et al.* (2001) reported on a combined NIS and thy-roperoxidase (TPO) gene co-transfer strategy in order to maximise intracellular radioiodide retention. This was based on the principle that TPO catalyzes iodination of proteins and promotes iodide retention within thyroid tissue. Trans-fection of NSCLC cells with both human NIS and TPO genes resulted in an increase in radioiodide uptake and retention and enhanced tumour cell apoptosis compared to isolated NIS gene delivery [173]. In contrast, Boland *et al.* (2002) did not obtain a significant increase in the iodide retention time in SiHa human cervix tumour cells, even though the production of an enzymatically active TPO was tested and a significant increase in iodide organification was observed in the targeted cells [174]. This may not be all that surprising since the effectiveness of TPO-mediated iodide organification in the normal thyroid gland is related to the presence of a follicular architecture and the presence

of the colloid protein (thyroglobulin). In contrast, extrathyroidal tissues are deficient in either of these mechanisms. Therefore, combined NIS and TPO delivery is unlikely to confer a significant advantage in terms of prolongation of iodide retention in this situation.

Smit *et al.* (2006) evaluated the effect of a low-iodine diet and thyroid ablation on *in vivo* radioiodide accumulation in NIS-transfected follicular thyroid carcinoma cell line xenografts (F TC133-NIS30). Radioiodide ( $^{131}\text{I}$ ) half-life in FTC133-NIS30 tumours was 3.8 hours compared to 26.3 hours in thyroid-ablated mice kept on a low-iodide diet, leading to a much higher area under the time-radioactivity curve. Experimental radioiodide therapy with 2 mCi (74 MBq) in thyroid-ablated nude mice, kept on a low-iodide diet, delayed tumour development with a calculated tumour dose of 32.2 Gy. The authors postulated dietary iodide modulation, combined with thyroid ablation, as one of the possible ways of overcoming the short half-life of radioiodide observed following exogenous NIS gene therapy [175]. However, the limited applicability of this strategy in the clinical situation is likely to reduce the translational potential and hinder its further progress and development.

### Alternative Therapeutic Radioisotopes for Use in NIS Gene Therapy

Investigators have also looked at optimising the cytotoxic response following NIS gene transfer using alternative radioisotopes. In addition to pertechnetate ( $^{99\text{m}}\text{TcO}_4^-$ ) and iodide radioisotopes ( $^{123}\text{I}$  and  $^{131}\text{I}$ ), perrhenates ( $^{188}\text{ReO}_4^-$  and  $^{186}\text{ReO}_4^-$ ) are important therapeutic substrates of NIS.  $^{188}\text{Re}$  is a powerful  $\beta$ -emitting radioisotope with a half-life of 16.7 hours and a minimum electron energy of 0.528 MeV, that is approximately 7 times more potent than  $^{131}\text{I}$  (0.068 MeV) and effective over a higher tissue range (23–32 mm). This combined with the shorter half-life (17 hours vs 8 days for  $^{131}\text{I}$ ) makes it an attractive option for the treatment of NIS-transduced non-thyroidal tumours. The favourable energy characteristics of rhenium isotopes are likely to be associated with higher absorbed doses. This has been previously demonstrated in an endogenously NIS-expressing breast cancer model, where  $^{188}\text{Re}$  administration was associated with upto 4.5-fold higher radiation dose per MBq of radioisotope compared to  $^{131}\text{I}$  [176]. In keeping with the above observation, rhenium was associated with superior survival in rats bearing NIS-transduced F 98/hNIS gliomas, compared to  $^{131}\text{I}$  [177].

Furthermore, rhenium is not retained or organified by the thyroid gland, which alongside the shorter half-life should substantially reduce the risk of post-treatment hypothyroidism. Zuckier *et al.* (2004) characterised the kinetics and comparative biodistribution of perrhenate and iodide in healthy CD1 mice and showed marked similarity. However, rhenium uptake in the normal thyroid had started to diminish at 19 hours, compared to the rising uptake of iodide secondary to iodide organification [178]. Dadachova *et al.* (2005) reported on a study that compared the therapeutic effects of rhenium ( $^{188}\text{Re}$ ) and radioiodide ( $^{131}\text{I}$ ) in PyMT mice bearing mammary cancer xenografts. Mice were administered 2 doses (1.5 mCi each) of one of the two isotopes a week apart followed by assessment of their effects on tumour growth and thyroid function. Tumour growth was significantly inhibited in both the groups compared with the untreated control. However, there was significant reduction in the re-growth of the tumours in the rhenium-treated group compared with the  $^{131}\text{I}$  group. More importantly, rhenium was associated with normal thyroid function compared to undetectable thyroid hormone T3/T4 levels in the  $^{131}\text{I}$ -treated group [179]. More recently, Willhauck *et al.* (2007) reported on a study aimed at assessing the therapeutic efficiency of rhenium in stably transfected LNCaP cells expressing NIS regulated by the PSA promoter (NP-1). NP-1 cell xenografts in nude mice accumulated 8–16% of the injected dose (ID)/g of  $^{188}\text{Re}$ , with a biological half-life of 12.9 hours. This resulted in a 4.7-fold increase in the tumour absorbed dose ( $0.45\text{ Gy MBq}^{-1}$ ) as compared with  $^{131}\text{I}$ . The therapeutic effect of rhenium was significantly enhanced in larger tumours as

compared to  $^{131}\text{I}$  (average tumour volume reduction of 86% vs 75%), which is possibly a reflection of the higher range of beta particulate emission from rhenium. These results show that rhenium may offer significant therapeutic advantages over radioiodide, especially for the management of larger tumours [180].

Astatide ( $^{211}\text{At}$ ) is an  $\alpha$ -emitting radiohalide characterized by a short physical half-life of 7.2 hours. Alpha particles have energies ranging from 5–9 MeV, with corresponding tissue ranges of 5–10 cell diameters, and deposit 80–100 keV/ $\mu\text{m}$  along most of their track (rate of energy deposition increases to 300 keV/ $\mu\text{m}$  at the end of the track – the so-called Bragg peak). The decay of  $^{211}\text{At}$  results in the emission of  $\beta$ -particles with a mean linear energy transfer (LET) of 97 keV/ $\mu\text{m}$  that is approximately 500 times more potent than the corresponding beta particulate emission of  $^{131}\text{I}$ . Car-lin *et al.* (2005) reported on a study aimed at assessing the *in vitro* cytotoxicity of  $^{211}\text{At}$  and  $^{131}\text{I}$  in NIS-transduced glioma cells. They employed a first-order pharmacokinetic model to simulate the closed compartment system of medium and cells. Monte Carlo transport methods were then used to estimate the absorbed dose from the cumulated activity concentrations in the medium and cells. The absorbed doses per unit administered activity were 54- to 65- fold higher for  $^{211}\text{At}$  compared to  $^{131}\text{I}$  and that translated into superior cytotoxicity assessed by clonogenic assay. However, NIS-independent (non-specific) binding of  $^{211}\text{At}$  was higher than that of  $^{131}\text{I}$ , therefore yielding a lower absorbed dose ratio between NIS-transduced and non-transduced cells [181]. This non-specific binding of astatine may have detrimental effects on the therapeutic index and may offset any potential advantage. Petrich *et al.* (2006), reported on an *in vivo* study of astatine in mice harboring rapidly growing tumours established from a papillary thyroid carcinoma cell line genetically modified to express NIS (K1-NIS). Mice ( $n=25$ ) then received intraperitoneal injections of 1.0, 0.5 and 1.0 MBq of  $^{211}\text{At}$  on days 0, 5 and 16, respectively. Within 3 months, astatine caused complete primary tumour eradication in all cases of K1-NIS tumour-bearing mice with no recurrences during a 1 year follow-up. The survival of astatine-treated mice was 96% at 6 months and 60% at 1 year [182]. Although, the use of astatine is a promising option, this is confounded by its limited availability and major safety, production and handling issues that are likely to have an adverse impact on its future development.

### Upregulation of NIS Expression

Uptake of radioisotope is a direct function of the level of NIS expression within the cell. Increased uptake of the relevant radioisotope secondary to higher levels of NIS protein will increase the area under the time-radioactivity curve. Therefore, strategies aimed at upregulating NIS expression should lead to superior cytotoxic effect, by virtue of exploitation of the above principle. The use of dexamethasone and retinoids to enhance endogenous NIS expression in breast cancer models has been previously discussed [119, 121]. This strategy has also been investigated following exogenous NIS transfer in breast and prostate cancer models. Spitzweg *et al.* (2003) examined the effect of ATRA on the regulation of PSA promoter-directed NIS expression and its therapeutic effectiveness in NIS-transfected LNCaP (NP-1) cells. ATRA induced 3-fold, 2.3-fold, and 1.45-fold increases in the levels of NIS mRNA, protein and iodide uptake, respectively. Interestingly, the effect of ATRA on NIS upregulation was androgen-dependent as it was completely blocked in the presence of bicalutamide, a selective androgen antagonist. Following therapeutic radioiodide, 50% cell survival was observed in the NP-1 cells and this fell to 10% in the presence of ATRA [183]. In a more recent study, Lim *et al.* (2007) assessed the effects of ATRA on adenoviral-mediated NIS (CMV promoter) expression in MCF-7 cells. A dose-dependent increase in the level of NIS protein expression and iodide uptake was observed following treatment with ATRA [184]. ATRA-induced upregulation of NIS

expression appears to be a promising strategy for therapeutic optimisation following exogenous delivery. Further *in vivo* validation of the above results is awaited.

Radiation has been combined with CGT in the past with the aim of exploiting possible synergistic interactions between the two modalities. More specifically, radiation has been shown to enhance gene expression from both viral and non-viral vectors and increase the therapeutic efficacy of oncolytic viral therapy [185]. In the context of NIS gene delivery, it has recently been shown that external beam radiotherapy upregulates NIS expression from adenoviral vectors. Tumor cells were irradiated (0, 4 and 8 Gy) and infected at various time points with different multiplicities of infection (MOIs) (0.01, 0.1, 1 and 10) of adenoviral vectors expressing NIS under CMV or telomerase promoters (hTR, hTERT). Radiation-induced upregulation of NIS expression was radiation dose-dependent and more pronounced at lower MOIs, but was independent of the promoter. The effect of tumor cell irradiation on the time course of transgene expression from Ad-hTR-NIS was also assessed. The level of gene expression increased with time in irradiated cells, with higher levels of expression observed at later time points in the cells infected with the lower MOIs (0.01 and 0.1) of virus. At these lower MOIs, radioiodide uptake was at its greatest level at 144 hours in cells irradiated to 8 Gy and this contrasted sharply with the falling levels of gene expression in unirradiated cells at this time [186]. Using GFP and luciferase reporters, the same authors demonstrated that maintenance of double-stranded DNA breaks was responsible, at least in part, for radiation-induced upregulation of gene expression from adenoviral vectors [187]. Specifically, inhibitors of ataxia telangiectasia mutated (ATM)-, poly-(ADP-ribose) polymerase (PARP)- and DNA protein kinase (DNA-PK)-mediated DNA repair were shown to maintain double-stranded DNA breaks (as measured by  $\gamma$ H2AX foci) by fluorescent activated cell sorting and microscopy. Inhibition of DNA repair was associated with increased GFP expression from a replication-defective adenoviral vector (Ad-CMV-GFP) and radiation-induced upregulation of gene expression was abrogated by inhibitors of MAPK (PD980059, U0126) and PI-3K (LY294002), but not by p38 MAPK inhibition. *In vivo* administration of a water soluble DNA-PK inhibitor (KU0060648) was shown to maintain luciferase expression in HCT116 xenografts after intratumoral delivery of Ad-RSV-Luc. Subsequent studies have shown similar effects for NIS-expressing adenoviral vectors (Hingorani *et al.* unpublished observations).

### Radiosensitisation During NIS Gene Therapy

The therapeutic response to NIS-mediated  $^{131}\text{I}$  therapy may also be optimised with the use of radiosensitising agents aimed at enhancing the biological response (Fig. 4). The cytotoxic effect following radioisotope therapy, as with other forms of ionising radiation, depends primarily on the number and extent of lethal and sub-lethal DNA damaging events (double-strand breaks (DSB)) acquired prior to the efflux of radioisotope. The probability of acquiring an irreparable lethal DNA lesion increases in direct proportion with the time spent by the radioisotope within the cell. Furthermore, the therapeutic response depends on fidelity of the available cellular DNA repair pathways that can repair some of the sublethal damage acquired by the cell. This holds especially true for  $\beta$ -emitting radioisotopes that have relatively low LET values (0.2 keV/ $\mu\text{m}$ ) and, thus, a low ionising potential. Cell death following administration of  $\beta$ -emitting radioisotopes is due to radioactive decay within the primary cell (self-dose) or decay within the neighbouring cells (cross-fire). In either case, the low LET of the  $\beta$  particles may necessitate several of these particles (20,000 in one estimate) to traverse the cell nucleus in order to ensure DNA lethality and cell death [188]. However,  $\beta$  particulate irradiation is associated with a high probability of sub-lethal DNA lesions and this explains the linear-quadratic distribution of their logarithmic dose-response survival curves [188]. In contrast,  $\alpha$  particles are a form of high LET radiation (70–100 keV/ $\mu\text{m}$ ) and this significantly increases the probability of lethal DNA damage following their

application. In turn, this explains the linear distribution of their logarithmic dose-response curves. Previous studies have shown that traversal of 1–4  $\alpha$  particles through a mammalian cell nucleus may be sufficient to kill the cell [189–191].

Despite their favourable physical characteristics, the relative unavailability of  $\alpha$ -emitting radioisotopes makes their routine use unlikely. The therapeutic radioisotope most commonly employed in previous studies of NIS gene therapy has been the widely available  $\beta$ -emitting radioiodide ( $^{131}\text{I}$ ). The therapeutic limitations of  $^{131}\text{I}$  may be somewhat masked during its use for the treatment of thyroid cancer, because of the prolonged effective half-life secondary to retention and organification within the thyroid gland. This may not hold true when  $^{131}\text{I}$  is used for the treatment of non-thyroid cancer and may necessitate administration of an unusually high dose of the radioisotope for a clinically relevant dose of radiation to be delivered. However, it may be possible to enhance the biological effect of  $^{131}\text{I}$  by inhibiting the repair of sub-lethal DSB generated during its use. This may potentially overcome some of the perceived drawbacks of  $^{131}\text{I}$  therapy in the management of NIS-transduced non-thyroid cancer. This will certainly be an interesting area to explore in further studies.

## NIS AS REPORTER GENE

One of the main advantages of NIS gene is its applicability as a reporter gene that may be employed for real-time non-invasive assessment of the biodistribution, gene expression and replication of various vector systems [141]. Most commonly, NIS gene expression has been mapped using pertechnetate ( $^{99\text{m}}\text{TcO}_4^-$ ) or iodide ( $^{123}\text{I}$ )-based scintigraphic techniques with conventional gamma camera imaging [138, 150–152] or SPECT/CT [153]. Scintigraphic assessment enables estimation of the level of radioisotope uptake and the effective half-life within the NIS-transduced tumour, which may then be employed to provide reliable estimates of the tumour absorbed dose. The reporter function of NIS can, therefore, be an extremely important tool for appropriate dosimetric assessment in NIS-based therapeutic studies [192]. NIS has also been employed to map the replication of various viral vectors, including oncolytic adenovirus [154] and measles virus [159].

NIS-based  $^{99\text{m}}\text{TcO}_4^-$  scintigraphy was employed to assess the real-time *in vivo* biodistribution, in dogs, of a RCAV vector incorporating NIS and also expressing the CD/HSV- $\text{tk}_{\text{mut}}$  gene. Using high-resolution autoradiography it was possible to obtain an accurate 3D-reconstruction of the distribution of gene expression that enabled quantitation with sub-millimetre resolution. The authors conferred the term ‘GENIS’ (gene expression of Na/I symporter) to this NIS-based imaging protocol [193]. The same group has also reported the use of GENIS as a means of non-invasively monitoring viral gene expression in men with clinically localized prostate cancer. Patients received an intraprostatic injection of Ad5-yCD/mutTK(SR39)rep-hNIS and NIS gene expression was imaged by  $^{99\text{m}}\text{TcO}_4^-$  scintigraphy using single photon emission-computed tomography (SPECT). Gene expression was detected in the prostate in seven of nine patients at  $1 \times 10^{12}$  virus particles (vp) but not at the  $1 \times 10^{11}$  dose level. The volume and total amount of gene expression was quantified by SPECT and showed that, following injection of  $1 \times 10^{12}$  vp in 1 ml, gene expression volume (GEV) increased to a mean of  $6.6 \text{ cm}^3$ , representing 18% of the total prostate volume. GEV and intensity peaked 1–2 days after the adenovirus injection and was detectable in the prostate for up to 7 days. Whole-body imaging demonstrated no evidence of extraprostatic dissemination of the adenovirus [194].

## CONCLUSION

The rapid advances that have been made in the last decade in our understanding of the biology of NIS mean that NIS-mediated radioisotope therapy may represent an important

therapeutic strategy for the treatment of non-thyroid cancers. As such, it is possible that the therapeutic experience of controlling and curing metastatic thyroid cancer may eventually be extended to other cancer types. However, before this goal can be realised, a great deal of translational research will be needed. Key steps in the process will include optimisation of gene delivery and expression, selection of the most appropriate radioisotopes for imaging and therapy and evaluation of combination regimens in which NIS-mediated radioisotope therapy augments the activity of standard anti-tumor therapies. This latter point is particularly important since it is unlikely that NIS will be capable of acting as a stand-alone therapy in any of the common tumour types. The next decade is likely to see significant research activity in this exciting field of gene therapy.

## Acknowledgments

Supported in part by a grant from the National Institutes of Health (R01 CA107082).

## ABBREVIATIONS

<b>Ad-CEA-NIS</b>	adenovirus expressing NIS under the control of a carcinoembryonic antigen promoter
<b>Ad-CMV-NIS</b>	adenovirus expressing NIS under the control of a cytomegalovirus promoter
<b>ATM</b>	ataxia telangiectasia mutated
<b>ATRA</b>	all-trans retinoic acid
<b>CEA</b>	carcinoembryonic antigen
<b>CGT</b>	cancer gene therapy
<b>DNA-PK</b>	deoxyribonucleic acid protein kinase
<b>DUOX2</b>	dual oxidase-2
<b>ER</b>	oestrogen receptor
<b>GBq</b>	gigabecquerels
<b>GFP</b>	green fluorescent protein
<b>HDAC</b>	histone deacetylase
<b>IFN-<math>\gamma</math></b>	interferon gamma
<b>IL1-<math>\alpha</math></b>	interleukin-1 alpha
<b>IL1-<math>\beta</math></b>	interleukin-1 beta
<b>IL6</b>	interleukin 6
<b>LET</b>	linear energy transfer
<b>MBq</b>	megabecquerels
<b>MOI</b>	multiplicity of infection
<b>MTC</b>	medullary thyroid cancer
<b>MV-NIS</b>	measles virus expressing NIS
<b>NIS</b>	sodium iodide symporter
<b>NPT</b>	sodium/praline transporter

<b>PARP</b>	poly-(ADP ribose) polymerase
<b>PI-3K</b>	phosphatidylinositol-3 kinase
<b>PKA</b>	protein kinase A
<b>PKC</b>	protein kinase C
<b>PPAR-<math>\gamma</math></b>	peroxisome proliferator-activated receptor gamma
<b>PSA</b>	prostate specific antigen
<b>PTU</b>	propylthiouracil
<b>RA</b>	retinoic acid
<b>RAR</b>	retinoic acid receptor
<b>RARE</b>	retinoic acid response element
<b>RCAV</b>	replication-competent adenovirus
<b>RIBBE</b>	radiation-induced biological bystander effect
<b>ROS</b>	reactive oxygen species
<b>RT-PCR</b>	reverse transcription polymerase chain reaction
<b>RXR</b>	retinoid X receptor
<b>SGLT</b>	sodium/glucose co-transporter
<b>SMCT</b>	sodium/monocarboxylate transporter
<b>SMIT</b>	sodium/myo-inositol transporter
<b>SMVT</b>	sodium/multivitamin transporter
<b>SPECT/CT</b>	single photon emission computed tomography/computed tomography
<b>SSF</b>	sodium/solute symporter family
<b>Tg</b>	thyroglobulin
<b>TGF-<math>\beta</math></b>	transforming growth factor beta
<b>TNF-<math>\alpha</math></b>	tumour necrosis factor alpha
<b>TNF-<math>\beta</math></b>	tumour necrosis factor beta
<b>TPO</b>	thyroperoxidase
<b>TSH</b>	thyroid stimulating hormone
<b>T3</b>	tri-iodothyronine
<b>T4</b>	tetra-iodothyronine
<b>VPA</b>	valproic acid

## REFERENCES

1. Dohan O, De la Vieja A, Paroder V, Riedel C, Artani M, Reed M, Ginter CS, Carrasco N. The sodium/iodide symporter (NIS): characterization, regulation, and medical significance. *En-docr. Rev.* 2003; 24:48–77.
2. Haq MS, Harmer C. Thyroid cancer: an overview. *Nucl. Med. Commun.* 2004; 25:861–867. [PubMed: 15319589]

3. Baumann E. Uber den Jodgehalt der Schilddrusen von Menchen und tieren. Hoppe-Seyler 's Zeitschrift fur Physiologische Chemie. 1986; 22:1–17.
4. Spitzweg C, Harrington KJ, Pinke LA, Vile RG, Morris JC. Clinical review 132: The sodium iodide symporter and its potential role in cancer therapy. *J. Clin. Endocrinol. Metab.* 2001; 86:3327–3335. [PubMed: 11443208]
5. Eskandari S, Loo DD, Dai G, Levy O, Wright EM, Carrasco N. Thyroid Na<sup>+</sup>/I<sup>-</sup> symporter Mechanism, stoichiometry, and specificity. *J. Biol. Chem.* 1997; 272:27230–27238. [PubMed: 9341168]
6. Scott DA, Wang R, Kreman TM, Sheffield VC, Karniski LP. The Pendred syndrome gene encodes a chloride-iodide transport protein. *Nat. Genet.* 1999; 21:440–443. [PubMed: 10192399]
7. Dohán O, Portulano C, Basquin C, Reyna-Neyra A, Amzel LM, Carrasco N. The Na<sup>+</sup>/I<sup>-</sup> symporter (NIS) mediates electroneutral active transport of the environmental pollutant perchlorate. *Proc. Natl. Acad. Sci. USA.* 2007; 104:20250–20255. [PubMed: 18077370]
8. Ris-Stalpers C. Physiology and pathophysiology of the DUOXes. *Antioxid Redox Signal.* 2006; 8:1563–1572. [PubMed: 16987011]
9. Dai G, Levy O, Carrasco N. Cloning and characterization of the thyroid iodide transporter. *Nature.* 1996; 379:458–460. [PubMed: 8559252]
10. Smanik PA, Liu Q, Furminger TL, Ryu K, Xing S, Mazzaferri EL, Jhiang SM. Cloning of the human sodium iodide symporter. *Biochem. Biophys. Res. Commun.* 1996; 226:339–345. [PubMed: 8806637]
11. Levy O, Dai G, Riedel C, Ginter CS, Paul EM, Lebowitz AN, Carrasco N. Characterization of the thyroid Na/I symporter with an anti-COOH terminus antibody. *Proc. Natl. Acad. Sci. USA.* 1997; 94:5568–5573. [PubMed: 9159113]
12. Smanik PA, Ryu KY, Theil KS, Mazzaferri EL, Jhiang SM. Expression, exonintron organization, and chromosome mapping of the human sodium iodide symporter. *Endocrinology.* 1997; 138:3555–3558. [PubMed: 9231811]
13. Fujiwara H, Tatsumi K, Miki K, Harada T, Miyai K, Takai S, Amino N. Congenital hypothyroidism caused by a mutation in the Na<sup>+</sup>/I<sup>-</sup> symporter. *Nat. Genet.* 1997; 16:124–125. [PubMed: 9171822]
14. De la Vieja A, Reed MD, Ginter CS, Carrasco N. Amino acid residues in transmembrane segment IX of the Na<sup>+</sup>/I<sup>-</sup> symporter play a role in its Na<sup>+</sup> dependence and are critical for transport activity. *J. Biol. Chem.* 2007; 282:25290–25298. [PubMed: 17606623]
15. Dohán O, Gavrielides MV, Ginter C, Amzel LM, Carrasco N. Na<sup>+</sup>/I<sup>-</sup> symporter activity requires a small and uncharged amino acid residue at position 395. *Mol. Endocrinol.* 2002; 16:1893–1902. [PubMed: 12145342]
16. Ohno M, Zannini M, Levy O, Carrasco N, Di Lauro R. The paired-domain transcription factor Pax8 binds to the upstream enhancer of the rat sodium/iodide symporter gene and participates in both thyroid-specific and cyclic-AMP-dependent transcription. *Mol. Cell. Biol.* 1999; 19:2051–2060. [PubMed: 10022892]
17. Cass LA, Summers SA, Prendergast GV, Backer JM, Birnbaum MJ, Meinkoth JL. Protein kinase A-dependent and -independent signaling pathways contribute to cyclic AMP-stimulated proliferation. *Mol. Cell Biol.* 1999; 19:5882–5891. [PubMed: 10454535]
18. Armstrong R, Wen W, Meinkoth J, Taylor S, Montminy M. A refractory phase in cyclic AMP-responsive transcription requires down regulation of protein kinase A. *Mol. Cell. Biol.* 1995; 15:1826–1832. [PubMed: 7862172]
19. Taki K, Kogai T, Kanamoto Y, Hershman JM, Brent GA. A thyroid-specific far upstream enhancer in the human sodium/iodide symporter gene requires Pax-8 binding and cyclic adenosine 3', 5'-monophosphate response element-like sequence binding proteins for full activity and is differentially regulated in normal and thyroid cancer cells. *Mol. Endocrinol.* 2002; 16:2266–2282. [PubMed: 12351692]
20. Iacovelli L, Capobianco L, Salvatore L, Sallèse M, D'Ancona G, De Blasi A. Thyrotropin activates mitogen-activated protein kinase pathway in FRTL-5 by a cAMP-dependent protein kinase A-independent mechanism. *Mol. Pharmacol.* 2001; 60:924–933. [PubMed: 11641420]

21. Chun JT, Di Dato V, D'Andrea B, Zannini M, Di Lauro R. The CRE-like element inside the 50-upstream region of the rat sodium/iodide symporter gene interacts with diverse classes of b-Zip molecules that regulate transcriptional activities through strong synergy with Pax-8. *Mol. Endocrinol.* 2004; 18:2817–2829. [PubMed: 15319451]
22. Correze C, Blondeau JP, Pomerance M. The thyrotropin receptor is not involved in the activation of p42/p44 mitogen-activated protein kinases by thyrotropin preparations in Chinese hamster ovary cells expressing the human thyrotropin receptor. *Thyroid.* 2000; 10:747–752. [PubMed: 11041451]
23. Medina DL, Santisteban P. Thyrotropin-dependent proliferation of *in vitro* rat thyroid cell systems. *Eur. J. Endocrinol.* 2000; 143:161–178. [PubMed: 10913934]
24. Pomerance M, Abdullah HB, Kamerji S, Correze C, Blondeau JP. Thyroid-stimulating hormone cyclic AMP activate p38 mitogen-activated protein kinase cascade Involvement of protein kinase A, rac1 and reactive oxygen species. *J. Biol. Chem.* 2000; 275:40539–40548. [PubMed: 11006268]
25. Garcia B, Santisteban P. PI3K is involved in the IGF-1 inhibition of TSH-induced sodium/iodide symporter gene expression. *Mol. Endocrinol.* 2002; 16:342–352. [PubMed: 11818505]
26. Cass LA, Meinkoth JL. Ras signaling through PI3K confers hormone-independent proliferation that is compatible with differentiation. *Oncogene.* 2000; 19:924–932. [PubMed: 10702801]
27. Pekary AE, Hershman JM. Tumor necrosis factor, ceramide, transforming growth factor-beta1, and aging reduce Na<sup>+</sup>/I<sup>-</sup> sym-porter messenger ribonucleic acid levels in FRTL-5 cells. *Endocrinology.* 1998; 139:703–712. [PubMed: 9449644]
28. Pekary AE, Levin SR, Johnson DG, Berg L, Hershman JM. Tumor necrosis factor-alfa (TNF-alfa) and transforming growth factor beta1 (TGF-beta1) inhibit the expression and activity of Na<sup>+</sup>/K<sup>+</sup> +ATPase in FRTL-5 rat thyroid cells. *J. Interferon Cytokine Res.* 1997; 4:185–195. [PubMed: 9142647]
29. Costamagna E, Garcia B, Santisteban P. The functional interaction between the paired domain transcription factor Pax8 and Smad3 is involved in transforming growth factorbeta repression of the sodium/iodide symporter gene. *J. Biol. Chem.* 2004; 279:3439–3446. [PubMed: 14623893]
30. Behr M, Schmitt TL, Espinoza CR, Loos U. Cloning of a functional promoter of the human sodium/iodide symporter gene. *Biochem. J.* 1998; 331:359–363. [PubMed: 9531470]
31. Ryu KY, Tong Q, Jhiang SM. Promoter characterization of the human Na/I symporter. *J. Clin. Endocrinol. Metab.* 1998; 83:3247–3251. [PubMed: 9745437]
32. Tong Q, Ryu KY, Jhiang SM. Promoter characterization of the rat Na/I symporter gene. *Biochem. Biophys. Res. Commun.* 1997; 239:34–41. [PubMed: 9345265]
33. Endo T, Kaneshige M, Nakazato M, Ohmori M, Harri N, Onaya T. Thyroid transcription factor-1 activates the promoter activity of rat Na/I symporter gene. *Mol. Endocrinol.* 1997; 11:1747–1755. [PubMed: 9328356]
34. Ohmori M, Endo T, Harri N, Onaya T. A novel thyroid transcription factor is essential for thyrotropin induced upregulation of Na/I symporter gene expression. *Mol. Endocrinol.* 1998; 12:727–736. [PubMed: 9605935]
35. Schmitt LT, Espinoza CR, Loos U. Characterization of a thyroid-specific and cyclic adenosine monophosphate-responsive enhancer far upstream from the human sodium iodide symporter gene. *Thyroid.* 2002; 12:273–278. [PubMed: 12034050]
36. Vassart G, Dumont JE. The thyrotropin receptor and the regulation of thyrocyte function and growth. *Endocr. Rev.* 1992; 13:596–611. [PubMed: 1425489]
37. Laglia G, Zeiger MA, Leipricht A, Caturegli P, Levine MA, Kohn LD, Saji M. Increased cyclic adenosine 3',5'-monophosphate inhibits G protein-coupled activation of phospholipase C in rat FRTL-5 thyroid cells. *Endocrinology.* 1996; 137:3170–3176. [PubMed: 8754735]
38. Saito T, Endo T, Kawaguchi A, Ikeda M, Nakazato M, Kogai T, Onaya T. Increased expression of the Na/I symporter in cultured human thyroid cells exposed to thyrotropin and in Graves' thyroid tissue. *J. Clin. Endocrinol. Metab.* 1997; 82:3331–3336. [PubMed: 9329364]
39. Uyttersprot N, Pelgrims N, Carrasco N, Gervy C, Maenhaut C, Dumont JE, Miot F. Moderate doses of iodide *in vivo* inhibit cell proliferation and the expression of thyroperoxidase and Na/I symporter mRNAs in dog thyroid. *Mol. Cell. Endocrinol.* 1997; 131:195–203. [PubMed: 9296378]

40. Levy O, De la Vieja A, Ginter CS, Riedel C, Dai G, Carrasco N. N-linked glycosylation of the thyroid Na<sup>+</sup>/I<sup>-</sup> symporter (NIS) Implications for its secondary structure model. *J. Biol. Chem.* 1998; 273:22657–22663. [PubMed: 9712895]
41. Riedel C, Levy O, Carrasco N. Post-transcriptional regulation of the sodium/iodide symporter by thyrotropin. *J. Biol. Chem.* 2001; 276:21458–21463. [PubMed: 11290744]
42. Kogai T, Endo T, Saito T, Miyazaki A, Kawaguchi A, Onaya T. Regulation by thyroid-stimulating hormone of sodium/iodide symporter gene expression and protein levels in FRTL-5 cells. *Endocrinology.* 1997; 138:2227–2232. [PubMed: 9165005]
43. Paire A, Bernier-Valentin F, Selmi-Ruby S, Rousset B. Characterization of the rat thyroid iodide transporter using anti-peptide antibodies. *J. Biol. Chem.* 1997; 272:18245–18249. [PubMed: 9218462]
44. Dohán A, Carrasco N. Advances in Na<sup>+</sup>/I<sup>-</sup> symporter (NIS) research in the thyroid and beyond. *Mol. Cell. Endocrinol.* 2003; 213:59–70. [PubMed: 15062574]
45. Kogai T, Curcio F, Hyman S, Cornford EM, Brent GA, Hershman JM. Induction of follicle formation in long-term cultured normal human thyroid cells treated with thyrotropin stimulates iodide uptake but not sodium/iodide symporter messenger RNA and protein expression. *J. Endocrinol.* 2000; 167:125–135. [PubMed: 11018760]
46. Kaminsky SM, Levy O, Salvador C, Dai G, Carrasco N. Na/I symporter activity is present in membrane vesicles from thyrotropin-deprived non-I transporting cultured thyroid cells. *Proc. Natl. Acad. Sci. USA.* 1994; 91:3789–3793. [PubMed: 8170988]
47. Yokomori N, Tawata M, Saito T, Shimura H, Onaya T. Regulation of the rat thyrotropin receptor gene by the methylation-sensitive transcription factor GA-binding protein. *Mol. Endocrinol.* 1998; 12:1241–1249. [PubMed: 9717849]
48. Glavy JS, Wu SM, Wang PJ, Orr GA, Wolkoff AW. Down-regulation by extracellular ATP of rat hepatocyte organic anion transport is mediated by serine phosphorylation of oatp1. *J. Biol. Chem.* 2000; 275:1479–1484. [PubMed: 10625701]
49. Krantz DE, Waites C, Oorschot V, Liu Y, Wilson RI, Tan PK, Klumperman J, Edwards RH. A phosphorylation site regulates sorting of the vesicular acetylcholine transporter to dense core vesicles. *J. Cell. Biol.* 2000; 149:379–396. [PubMed: 10769030]
50. Ramamoorthy S, Blakely RD. Phosphorylation and sequestration of serotonin transporters differentially modulated by psychostimulants. *Science.* 1999; 285:763–766. [PubMed: 10427004]
51. De la Vieja A, Dohán O, Levy O, Carrasco N. Molecular analysis of the sodium/iodide symporter: impact on thyroid and ex-thyroid pathophysiology. *Physiol. Rev.* 2000; 80:1083–1095. [PubMed: 10893432]
52. Msaouel P, Iankov ID, Allen C, Aderca I, Federspiel MJ, Tindall DJ, Morris JC, Koutsilieris M, Russell SJ, Galanis E. *Mol. Ther.* 2009; 17:2041–2048. [PubMed: 19773744]
53. Fanning AS, Anderson JM. PDZ domains: fundamental building blocks in the organization of protein complexes at the plasma membrane. *J. Clin. Invest.* 1999; 103:767–772. [PubMed: 10079096]
54. Perego C, Vanoni C, Villa A, Longhi R, Kaech SM, Frohli E, Hajnal A, Kim SK, Pietrini G. PDZ-mediated interactions retain the epithelial GABA transporter on the basolateral surface of polarized epithelial cells. *EMBO J.* 1999; 18:2384–2393. [PubMed: 10228153]
55. Marks MS, Ohno H, Kirchhausen T, Bonifacino JS. Protein sorting by tyrosine-based signals: adapting to the Ys and where-fores. *Trends Cell Biol.* 1997; 7:124–128. [PubMed: 17708922]
56. Piguet V, Gu F, Foti M, Demaurex N, Gruenberg J, Carpentier JL, Trono D. Nef-induced CD4 degradation: a diacidic-based motif in Nef functions as a lysosomal targeting signal through the binding of β-COP in endosomes. *Cell.* 1999; 97:63–73. [PubMed: 10199403]
57. Voorhees P, Deignan E, Van Donselaar E, Humphrey J, Marks MS, Peters PJ, Bonifacino JS. An acidic sequence within the cytoplasmic domain of furin functions as a determinant of trans-Golgi network localization and internalization from the cell surface. *EMBO J.* 1995; 14:4961–4975. [PubMed: 7588625]
58. Waites CL, Mehta A, Tan PK, Thomas G, Edwards RH, Krantz DE. An acidic motif retains vesicular monoamine transporter 2 on large dense core vesicles. *J. Cell Biol.* 2001; 152:1159–1168. [PubMed: 11257117]

59. Hertz S, Roberts A, Salter WT. Radioactive iodine as an indicator in thyroid physiology IV The metabolism of iodine in Graves' disease. *J. Clin. Invest.* 1942; 21:25–29. [PubMed: 16694887]
60. Lazar V, Bidart J-M, Caillou B, Mahe C, Lacroix L, Filetti S, Schlumberger M. Expression of the Na<sup>+</sup>/I<sup>-</sup> symporter gene in human thyroid tumors: a comparison study with other thyroid-specific genes. *J. Clin. Endocrinol. Metab.* 1999; 84:3228–3234. [PubMed: 10487692]
61. Trapasso F, Iuliano R, Chiefari E, Arturi F, Stella A, Filetti S, Fusco A, Russo D. Iodide symporter gene expression in normal and transformed rat thyroid cells. *Eur. J. Endocrinol.* 1999; 140:447–451. [PubMed: 10229912]
62. Park H-J, Kim JY, Park KY, Gong G, Hong SJ, Ahn I-M. Expression of human sodium iodide symporter mRNA in primary and metastatic papillary thyroid carcinomas. *Thyroid.* 2000; 10:211–217. [PubMed: 10779135]
63. Saito T, Endo T, Kawaguchi A, Ikeda M, Katoh R, Kawaoi A, Muramatsu A, Onaya T. Increased expression of the sodium/iodide symporter in papillary thyroid carcinomas. *J. Clin. Invest.* 1998; 101:1296–1300. [PubMed: 9525971]
64. Dohán O, Baloch Z, Bánrévi Z, Livolsi V, Carrasco N. Rapid communication: predominant intracellular overexpression of the Na<sup>(+)</sup>/I<sup>(-)</sup> symporter (NIS) in a large sampling of thyroid cancer cases. *J. Clin. Endocrinol. Metab.* 2001; 86:2697–2700. [PubMed: 11397873]
65. Wolff J, Chaikoff IL. Plasma inorganic iodide as a homeostatic regulator of thyroid function. *J. Biol. Chem.* 1948; 174:555–564. [PubMed: 18865621]
66. Raben MS. The paradoxical effect of thiocyanate and of thyrotropin on the organic binding of iodine by the thyroid in the presence of large amounts of iodide. *Endocrinology.* 1949; 45:296–304. [PubMed: 18140410]
67. Grollman EF, Smolar A, Ommaya A, Tombaccini D, Santisteban P. Iodine suppression of iodide uptake in FRTL-5 thyroid cells. *Endocrinology.* 1986; 118:2477–2482. [PubMed: 3009160]
68. Spitzweg C, Joba W, Morris JC, Heufelder AE. Regulation of sodium iodide symporter gene expression in FRTL-5 rat thyroid cells. *Thyroid.* 1999; 9:821–830. [PubMed: 10482376]
69. Eng PHK, Cardona GR, Fang SL, Previti M, Alex S, Carrasco N, Chin WW, Braverman LE. Escape from the acute Wolff-Chaikoff effect is associated with a decrease in thyroid sodium/iodide symporter messenger ribonucleic acid and protein. *Endocrinology.* 1999; 140:3404–3410. [PubMed: 10433193]
70. Eng PHK, Cardona GR, Previti MC, Chin WW, Braverman LE. Regulation of the sodium iodide symporter by iodide in FRTL-5 cells. *Eur. J. Endocrinol.* 2001; 144:139–144. [PubMed: 11182750]
71. Ajjan RA, Watson PF, Findlay C, Metcalfe RA, Crisp M, Ludgate M, Weetman AP. The sodium iodide symporter gene and its regulation by cytokines found in autoimmunity. *J. Endocrinol.* 1998; 158:351–358. [PubMed: 9846164]
72. Rasmussen AK, Kayser L, Feldt-Rasmussen U. Influence of tumor necrosis factor- $\alpha$  (TNF- $\alpha$ ), tumor necrosis factor- $\beta$  and interferon- $\gamma$ , separately and added together with interleukin-1 $\beta$ , on the function of cultured human thyroid cells. *J. Endocrinol.* 1994; 143:359–365. [PubMed: 7829998]
73. Caturegli P, Hejazi M, Suzuki K, Dohan O, Carrasco N, Kohn LD, Rose NR. Hypothyroidism in transgenic mice expressing IFN- $\gamma$  in the thyroid. *Proc. Natl. Acad. Sci. USA.* 2000; 97:1719–1724. [PubMed: 10677524]
74. Santoro M, Melillo RM, Grieco M, Berlingieri MT, Vecchio G, Fusco A. The TRK and RET tyrosine kinase oncogenes cooperate with ras in the neoplastic transformation of a rat thyroid epithelial cell line. *Cell Growth Differ.* 1993; 4:77–84. [PubMed: 8494786]
75. Knauf JA, Ouyang B, Croyle M, Kimura E, Fagin JA. Acute expression of RET/PTC induces isozyme-specific activation and subsequent downregulation of PKCepsilon in PCCL3 thyroid cells. *Oncogene.* 2003; 22:6830–6838. [PubMed: 14534528]
76. Mitsutake N, Knauf JA, Mitsutake S, Mesa C Jr, Zhang L, Fagin JA. Conditional BRAFV600E expression induces DNA synthesis, apoptosis, dedifferentiation, and chromosomal instability in thyroid PCCL3 cells. *Cancer Res.* 2005; 65:2465–2473. [PubMed: 15781663]
77. Riesco-Eizaguirre G, Gutierrez-Martinez P, Garcia-Cabezas M, Nistal M, Santisteban P. The oncogene BRAF<sup>V600E</sup> is associated with a high risk of recurrence and less differentiated papillary

thyroid carcinoma due to the impairment of  $\text{Na}^+/\text{I}^-$  targeting to the membrane. *Endocrine Rel. Cancer*. 2006; 13:257–269.

78. Schmutzler C, Winzer R, Meissner-Weigl J, Kohrle J. Retinoic acid increases sodium/iodide symporter mRNA levels in human thyroid cancer cell lines and suppresses expression of functional symporter in nontransformed FRTL-5 rat thyroid cells. *Biochem. Biophys. Res. Commun.* 1997; 240:832–838. [PubMed: 9398654]
79. Jeong H, Kim YR, Kim KN, Choe JG, Chung JK, Kim MK. Effect of all-trans retinoic acid on sodium/iodide symporter expression, radioiodine uptake and gene expression profiles in a human anaplastic thyroid carcinoma cell line. *Nucl. Med. Biol.* 2006; 33:875–882. [PubMed: 17045167]
80. Simon D, Korber C, Krausch M, Segering J, Groth P, Gorges R, Grunwald F, Muller-Gartner HW, Schmutzler C, Kohrle J, Roher HD, Reiners C. Clinical impact of retinoids in redifferentiation therapy of advanced thyroid cancer: final results of a pilot study. *Eur. J. Nucl. Med. Mol. Imag.* 2002; 29:775–782.
81. Marques AR, Espadinha C, Catarino AL, Moniz S, Pereira T, Sobrinho LG, Leite V. Expression of PAX8-PPAR gamma 1 rearrangements in both follicular thyroid carcinomas and adenomas. *J. Clin. Endocrinol. Metab.* 2002; 87:3947–3952. [PubMed: 12161538]
82. Castro P, Rebocho AP, Soares RJ, Magalhaes J, Roque L, Trovisco V, Vieira de Castro I, Cardoso-de-Oliveira M, Fon-seca E, Soares P, Sobrino-Simoes M. PAX8-PPARgamma rearrangement is frequently detected in the follicular variant of papillary thyroid carcinoma. *J. Clin. Endocrinol. Metab.* 2006; 91:213–220. [PubMed: 16219715]
83. Park JW, Zarnegar R, Kanauchi H, Wong MG, Hyun WC, Ginzinger DG, Lobo M, Cotter P, Duh QY, Clark OH. Troglitazone, the peroxisome proliferator-activated receptor-gamma agonist, induces antiproliferation and redifferentiation in human thyroid cancer cell lines. *Thyroid*. 2005; 15:222–231. [PubMed: 15785241]
84. Ohta K, Endo T, Haraguchi K, Hershman JM, Onaya T. Ligands for peroxisome proliferator-activated receptor gamma inhibit growth and induce apoptosis of human papillary thyroid carcinoma cells. *J. Clin. Endocrinol. Metab.* 2001; 86:2170–2177. [PubMed: 11344222]
85. Marks P, Rifkind RA, Richon VM, Breslow R, Miller T, Kelly WK. Histone deacetylases and cancer: causes and therapies. *Nat. Rev. Cancer*. 2001; 1:194–202. [PubMed: 11902574]
86. Kitazono M, Robey R, Zhan Z, Sarlis NJ, Skarulis MC, Aikou T, Bates S, Fojo T. Low concentrations of the histone deacetylase inhibitor, depsipeptide (FR901228), increase expression of the NaC/IK symporter and iodine accumulation in poorly differentiated thyroid carcinoma cells. *J. Clin. Endocrinol. Metab.* 2001; 86:3430–3435. [PubMed: 11443220]
87. Furuya F, Shimura H, Suzuki H, Taki K, Ohta K, Haraguchi K, Onaya T, Endo T, Kobayashi T. Histone deacetylase inhibitors restore radioiodide uptake and retention in poorly differentiated and anaplastic thyroid cancer cells by expression of the sodium/iodide symporter thyroperoxidase and thyroglobulin. *Endocrinology*. 2004; 145:2865–2875. [PubMed: 14976143]
89. Fortunati N, Catalano MG, Arena K, Brignardello E, Piove-san A, Boccuzzi G. Valproic acid induces the expression of the NaC/IK symporter and iodine uptake in poorly differentiated thyroid cancer cells. *J. Clin. Endocrinol. Metab.* 2004; 89:1006–1009. [PubMed: 14764827]
90. Shen WT, Wong TS, Chung WY, Wong MG, Kebebew E, Duh QY, Clark OH. Valproic acid inhibits growth, induces apoptosis, and modulates apoptosis-regulatory and differentiation gene expression in human thyroid cancer cells. *Surgery*. 2005; 138:979–985. [PubMed: 16360381]
91. Baylin SB. Tying it all together: epigenetics, genetics, cell cycle, and cancer. *Science*. 1997; 277:1948–1949. [PubMed: 9333948]
92. Venkataraman GM, Yatin M, Marcinek R, Ain KB. Restoration of iodide uptake in dedifferentiated thyroid carcinoma: relationship to human Na<sup>+</sup>/I<sup>-</sup> symporter gene methylation status. *J. Clin. Endocrinol. Metab.* 1999; 84:2449–2457. [PubMed: 10404820]
93. Neumann S, Schuchardt K, Reske A, Emmrich P, Paschke R. Lack of correlation for sodium iodide symporter mRNA and protein expression and analysis of sodium iodide symporter promoter methylation in benign cold thyroid nodules. *Thyroid*. 2004; 14:99–111. [PubMed: 15068624]
94. Ulianich L, Suzuki K, Mori A, Nakazato M, Pietrarelli M, Goldsmith P, Pacifico F, Consiglio E, Formisano S, Kohn LD. Follicular thyroglobulin (TG) suppression of thyroid-restricted genes

- involves the apical membrane asialoglycoprotein receptor and TG phosphorylation. *J. Biol. Chem.* 1999; 274:25099–25107. [PubMed: 10455190]
95. Furlanetto TW, Nguyen LQ, Jameson JL. Estradiol increases proliferation and down-regulates the sodium/iodide sym-porter gene in FRTL-5 cells. *Endocrinology.* 1999; 140:5705–5711. [PubMed: 10579335]
  96. Brown-Grant K. Extra-thyroidal iodide concentrating mechanisms. *Physiol. Rev.* 1961; 41:189–213.
  97. Carrasco N. Iodide transport in the thyroid gland. *Biochim. Bio-phys. Acta.* 1993; 1154:65–82.
  98. Halmi NS. Thyroidal iodide transport. *Vitam. Horm.* 1961; 19:133–163.
  99. Ajjan RA, Kamaruddin NA, Crisp M, Watson PF, Lud-gate M, Weetman AP. Regulation and tissue distribution of the human sodium iodide symporter gene. *Clin. Endocrinol. (Oxf).* 1998; 49:517–523. [PubMed: 9876351]
  100. Spitzweg C, Joba W, Eisenmenger W, Heufelder AE. Analysis of human sodium iodide symporter gene expression in extrathyroidal tissues and cloning of its complementary DNA from salivary gland, mammary gland, and gastric mucosa. *J. Clin. Endocrinol. Metab.* 1998; 83:1746–1751. [PubMed: 9589686]
  101. Cho JY, Leveille R, Kao R, Rousset B, Parlow AF, Burak WE Jr, Mazzaferri EL, Jhiang SM. Hormonal regulation of radioiodide uptake activity and Na<sup>+</sup>/I<sup>-</sup> symporter expression in mammary glands. *J. Clin. Endocrinol. Metab.* 2000; 85:2936–2943. [PubMed: 10946907]
  102. Spitzweg C, Dutton CM, Castro MR, Bergert ER, Goell-ner JR, Heufelder AE, Morris JC. Expression of the sodium iodide symporter in human kidney. *Kidney Int.* 2001; 59:1013–1023. [PubMed: 11231356]
  103. Taurog A, Dorris ML, Lamas L. Comparison of lactoperoxi-dase- and thyroid peroxidase-catalyzed iodination and coupling. *Endocrinology.* 1974; 94:1286–1294. [PubMed: 4856726]
  104. Tazebay UH, Wapnir IL, Levy O, Dohan O, Zuckier LS, Zhao QH, Deng HF, Amenta PS, Fineberg S, Pestell RG, Carrasco N. The mammary gland iodide transporter is expressed during lactation and in breast cancer. *Nat. Med.* 2000; 6:871–878. [PubMed: 10932223]
  105. Rillema JA, Yu TX, Jhiang SM. Effect of prolactin on sodium iodide symporter expression in mouse mammary gland ex-plants. *Am. J. Physiol. Endocrinol. Metab.* 2000; 279:E769–E772. [PubMed: 11001757]
  106. Jhiang SM, Cho JY, Ryu KY, DeYoung BR, Smanik PA, McGauchy VR, Fischer AH, Mazzaferri EL. An immu-nohistochemical study of Na<sup>+</sup>/I<sup>-</sup> symporter in human thyroid tissues and salivary gland tissues. *Endocrinology.* 1998; 139:4416–4419. [PubMed: 9751526]
  107. Vayre L, Sabourin JC, Caillou B, Ducreux M, Schlumberger M, Bidart JM. Immunohistochemical analysis of Na<sup>+</sup>/I<sup>-</sup> sym-porter distribution in human extra-thyroid tissues. *Eur. J. Endocrinol.* 1999; 141:382–386. [PubMed: 10526253]
  108. Wapnir IL, van de Rijn M, Nowels K, Amenta PS, Walton K, Montgomery K, Greco RS, Dohan O, Carrasco N. Immu-nohistochemical profile of the sodium/iodide symporter in thyroid, breast, and other carcinomas using high density tissue microarrays and conventional sections. *J. Clin. Endocrinol. Metab.* 2003; 88:1880–1888. [PubMed: 12679487]
  109. Moon DH, Lee SJ, Park KY, Park KK, Ahn SH, Pai MS, Chang H, Lee HK, Ahn IM. Correlation between <sup>99m</sup>Tc-pertechnetate uptake and expression of human sodium iodide symporter gene in breast tumor tissues. *Nucl. Med. Biol.* 2001; 28:829–834. [PubMed: 11578905]
  110. Wapnir IL, Goris M, Yudd A, Dohan O, Adelman D, Now-els K, Carrasco N. The Na<sup>+</sup>/I<sup>-</sup> symporter mediates iodide uptake in breast cancer metastases and can be selectively downregulated in the thyroid. *Clin. Cancer Res.* 2004; 10:4294–4302. [PubMed: 15240514]
  111. Knostman KA, McCubrey JA, Morrison CD, Zhang Z, Capen CC, Jhiang SM. PI3K activation is associated with in-tracellular sodium/iodide symporter protein expression in breast cancer. *BMC Cancer.* 2007; 7:137. [PubMed: 17651485]
  112. Kogai T, Schultz JJ, Johnson LS, Huang M, Brent GA. Retinoic acid induces sodium/iodide symporter gene expression and radioiodide uptake in the MCF-7 breast cancer cell line. *Proc. Natl. Acad. Sci. USA.* 2000; 97:8519–8524. [PubMed: 10890895]
  113. Kogai T, Kanamoto Y, Li AI, Che LH, Ohashi E, Taki K, Chandraratna RA, Saito T, Brent GA. Differential regulation of sodium/iodide symporter (NIS) gene expression by nuclear receptor

- ligands in MCF-7 breast cancer cells. *Endocrinology*. 2005; 146:3059–3069. [PubMed: 15817668]
114. Tanosaki S, Ikezoe T, Heaney A, Said JW, Dan K, Akashi M, Koeffler HP. Effect of ligands of nuclear hormone receptors on sodium/iodide symporter expression and activity in breast cancer cells. *Breast Cancer Res. Treat.* 2003; 79:335–345. [PubMed: 12846418]
115. Kogai T, Kanamoto Y, Che LH, Taki K, Moatamed F, Schultz JJ, Brent GA. Systemic retinoic acid treatment induces sodium/iodide symporter expression and radioiodide uptake in mouse breast cancer models. *Cancer Res.* 2004; 64:415–422. [PubMed: 14729653]
116. Agarwal C, Chandraratna RA, Johnson AT, Rorke EA, Eckert RL. AGN193109 is a highly effective antagonist of retinoid action in human ectocervical epithelial cells. *J. Biol. Chem.* 1996; 271:12209–12212. [PubMed: 8647816]
117. Blaner WS. Cellular metabolism and actions of 13-cis retinoic acid. *J. Am. Acad. Dermatol.* 2001; 45:S129–S135. [PubMed: 11606944]
118. Kogai T, Kanamoto Y, Brent GA. The modified firefly luciferase reporter gene (lucC) but not Renilla luciferase is induced by all-trans retinoic acid in MCF-7 breast cancer cells. *Breast Cancer Res. Treat.* 2003; 78:119–126. [PubMed: 12611464]
119. Dentice M, Luongo C, Elefante A, Romino R, Ambrosio R, Vitale M, Rossi G, Fenzi G, Salvatore D. Transcription factor Nkx-2.5 induces sodium/iodide symporter gene expression and participates in retinoic acid- and lactation-induced transcription in mammary cells. *Mol. Cell. Biol.* 2004; 24:7863–7877. [PubMed: 15340050]
120. Kogai T, Taki K, Brent GA. Enhancement of sodium/iodide symporter expression in thyroid and breast cancer. *Endocr. Relat. Cancer.* 2006; 13:797–826. [PubMed: 16954431]
121. Unterholzner S, Willhauck MJ, Cengic N, Schütz M, Göke B, Morris JC, Spitzweg C. Dexamethasone stimulation of retinoic acid-induced sodium iodide symporter expression and cyto-toxicity of 131-I in breast cancer cells. *J. Clin. Endocrinol. Metab.* 2006; 91:69–78. [PubMed: 16234306]
122. Willhauck MJ, Sharif-Samani B, Senekowitsch-Schmidtke R, Wunderlich N, Göke B, Morris JC, Spitzweg C. Functional sodium iodide symporter expression in breast cancer xenografts *in vivo* after systemic treatment with retinoic acid and dexamethasone. *Breast Cancer Res. Treat.* 2008; 109:263–272. [PubMed: 17636401]
123. Pasięka JL, McEwan AJ, Rorstad O. The palliative role of 131I-MIBG and 111-In-octreotide therapy in patients with metastatic progressive neuroendocrine neoplasms. *Surgery.* 2004; 136:1218–1226. [PubMed: 15657579]
124. Liepe K, Kotzerke J. A comparative study of 188Re-HEDP, 186Re-HEDP, 153Sm-EDTMP and 89Sr in the treatment of painful skeletal metastases. *Nucl. Med. Commun.* 2007; 28:623–630. [PubMed: 17625384]
125. Shelley MD, Mason MD. Radium-223 for men with hormone-refractory prostate cancer and bone metastases. *Lancet Oncol.* 2007; 8:564–567. [PubMed: 17613416]
126. Taggart D, Dubois S, Matthay KK. Radiolabeled metaiodo-benzylguanidine for imaging and therapy of neuroblastoma. *Q. J. Nucl. Med. Mol. Imaging.* 2008; 52:403–418. [PubMed: 19088694]
127. Illidge TM, Bayne MC. Antibody therapy of lymphoma. *Expert Opin. Pharmacother.* 2001; 2:953–961. [PubMed: 11585011]
128. Spitzweg C, Zhang S, Bergert ER, Castro MR, McIver B, Heufelder AE, Tindall DJ, Young CY, Morris JC. Prostate specific antigen (PSA) promoter-driven androgen-inducible expression of sodium iodide symporter in prostate cancer cell lines. *Cancer Res.* 1999; 59:2136–2141. [PubMed: 10232600]
129. Spitzweg C, O'Connor MK, Bergert ER, Tindall DJ, Young CY, Morris JC. Treatment of prostate cancer by radioiodine therapy after tissue-specific expression of the sodium iodide symporter. *Cancer Res.* 2000; 15:6526–6530. [PubMed: 11103823]
130. Spitzweg C, Dietz AB, O'Connor MK, Bergert ER, Tindall DJ, Young CY, Morris JC. *In vivo* sodium iodide symporter gene therapy of prostate cancer. *Gene Ther.* 2001; 8:1524–1531. [PubMed: 11704812]

131. Mothersill C, Seymour CB. Radiation-induced bystander effects-implications for cancer. *Nat. Rev. Cancer.* 2004; 4:158–164. [PubMed: 14964312]
132. Little JB, Azzam EI, De Toledo SM, Nagasawa H. Bystander effects: intercellular transmission of radiation damage signals. *Radiat. Prot. Dosimet.* 2002; 99:159–162.
133. Shimura H, Haraguchi K, Myazaki A, Endo T, Onaya T. Iodide uptake and experimental 131I therapy in transplanted undifferentiated thyroid cancer cells expressing the Na<sup>+</sup>/I<sup>-</sup> symporter gene. *Endocrinology.* 1997; 138:4493–4496. [PubMed: 9322970]
134. Riesco-Eizaguirre G, Santisteban P. A perspective view of sodium iodide symporter research and its clinical implications. *Eur. J. Endocrinol.* 2006; 155:495–512. [PubMed: 16990649]
135. Cho J-Y, Xing S, Liu X, Buckwalter TL, Hwa L, Sferra TJ, Chiu IM, Jhiang SM. Expression and activity of human Na<sup>+</sup>/I<sup>-</sup> symporter in human glioma cells by adenovirus-mediated gene delivery. *Gene Ther.* 2000; 7:740–749. [PubMed: 10822300]
136. Mandell RB, Mandell LZ, Link CJ. Radioisotope concentrator gene therapy using the sodium/iodide symporter gene. *Cancer Res.* 1999; 59:661–668. [PubMed: 9973215]
137. Boland A, Ricard M, Opolon P, Bidart JM, Yeh P, Filetti S, Schlumberger M, Perricaudet M. Adenovirus-mediated transfer of the thyroid sodium/iodide symporter gene into tumors for a targeted radiotherapy. *Cancer Res.* 2000; 60:3484–3492. [PubMed: 10910060]
138. Nakamoto Y, Saga T, Misaki T, Kobayashi H, Sato N, Ishimori T, Kosugi S, Sakahara H, Konishi J. Establishment and characterization of a breast cancer cell line expressing Na<sup>+</sup>/I<sup>-</sup> symporters for radioiodide concentrator gene therapy. *J. Nucl. Med.* 2000; 41:1898–1904. [PubMed: 11079502]
139. Cho Y-C, Shen DHY, Yang W, Williams B, Buckwalter TLF, La Perle KMD, Hinkle G, Pozderac R, Kloos R, Nagaraja HN, Barth RF, Jhiang SM. *In vivo* imaging and radioiodine therapy following sodium iodide symporter gene transfer in animal models of intracerebral gliomas. *Gene Ther.* 2002; 9:1139–1145. [PubMed: 12170377]
140. Kakinuma H, Bergert ER, Spitzweg C, Chevillie JC, Lieber MM, Morris JC. Probasin promoter (ARR(2)PB)-driven, prostate-specific expression of the human sodium iodide symporter (h-NIS) for targeted radioiodine therapy of prostate cancer. *Cancer Res.* 2003; 63:7840–7844. [PubMed: 14633711]
141. Sieger S, Jiang S, Schönsiegel F, Eskerski H, Kübler W, Altmann A, Haberkorn U. Tumour-specific activation of the sodium/iodide symporter gene under control of the glucose transporter gene 1 promoter (GTI-1.3). *Eur. J. Nucl. Med. Mol. Imaging.* 2003; 30:748–756. [PubMed: 12541134]
142. Haberkorn U, Kinscherf R, Kissel M, Kübler W, Mahmut M, Sieger S, Eisenhut M, Peschke P, Altmann A. Enhanced iodide transport after transfer of the human sodium iodide symporter gene is associated with lack of retention and low absorbed dose. *Gene Ther.* 2003; 10:774–780. [PubMed: 12704416]
143. Faivre J, Clerc J, Gérolami R, Hervé J, Longuet M, Liu B, Roux J, Moal F, Perricaudet M, Bréchet C. Long-term radioiodine retention and regression of liver cancer after sodium iodide symporter gene transfer in wistar rats. *Cancer Res.* 2004; 64:8045–8051. [PubMed: 15520214]
144. Gaut AW, Niu G, Krager KJ, Graham MM, Trask DK, Domann FE. Genetically targeted radiotherapy of head and neck squamous cell carcinoma using the sodium-iodide symporter (NIS). *Head Neck.* 2004; 26:265–271. [PubMed: 14999802]
145. Schipper ML, Weber A, Béhé M, Göke R, Joba W, Schmidt H, Bert T, Simon B, Arnold R, Heufelder AE, Behr TM. Radioiodide treatment after sodium iodide symporter gene transfer is a highly effective therapy in neuroendocrine tumor cells. *Cancer Res.* 2003; 63:1333–1338. [PubMed: 12649195]
146. Cengic N, Baker CH, Schütz M, Göke B, Morris JC, Spitzweg C. A novel therapeutic strategy for medullary thyroid cancer based on radioiodine therapy following tissue-specific sodium iodide symporter gene expression. *J. Clin. Endocrinol. Metab.* 2005; 90:4457–4464. [PubMed: 15941870]
147. Scholz IV, Cengic N, Baker CH, Harrington KJ, Maletz K, Bergert ER, Vile R, Göke B, Morris JC, Spitzweg C. Radioiodine therapy of colon cancer following tissue-specific sodium iodide symporter gene transfer. *Gene Ther.* 2005; 12:272–280. [PubMed: 15510175]

148. Dwyer RM, Bergert ER, O'Connor MK, Gendler SJ, Morris JC. *In vivo* radioiodide imaging and treatment of breast cancer xenografts after MUC1-driven expression of the sodium iodide symporter. *Clin. Cancer Res.* 2005; 11:1483–1489. [PubMed: 15746050]
149. Dwyer RM, Bergert ER, O'Connor MK, Gendler SJ, Morris JC. Adenovirus-mediated and targeted expression of the sodium-iodide symporter permits *in vivo* radioiodide imaging and therapy of pancreatic tumors. *Hum. Gene Ther.* 2006; 17:661–668. [PubMed: 16776574]
150. Dwyer RM, Bergert ER, O'Connor MK, Gendler SJ, Morris JC. Sodium iodide symporter-mediated radioiodide imaging and therapy of ovarian tumor xenografts in mice. *Gene Ther.* 2006; 13:60–66. [PubMed: 16121204]
151. Chen RF, Li ZH, Pan QH, Zhou JJ, Tang QB, Yu FY, Zhou QB, Wang J, Chen JS. *In vivo* radioiodide imaging and treatment of pancreatic cancer xenografts after MUC1 promoter-driven expression of the human sodium-iodide symporter. *Pancreatology.* 2007; 7:505–513. [PubMed: 17912014]
152. Spitzweg C, Baker CH, Bergert ER, O'Connor MK, Morris JC. Image-guided radioiodide therapy of medullary thyroid cancer after carcinoembryonic antigen promoter-targeted sodium iodide symporter gene expression. *Hum. Gene Ther.* 2007; 18:916–924. [PubMed: 17931047]
153. Willhauck MJ, Sharif Samani BR, Klutz K, Cengic N, Wolf I, Mohr L, Geissler M, Senekowitsch-Schmidtke R, Göke B, Morris JC, Spitzweg C. Alpha-fetoprotein promoter-targeted sodium iodide symporter gene therapy of hepatocellular carcinoma. *Gene Ther.* 2008; 15:214–223. [PubMed: 17989705]
154. Dwyer RM, Schatz SM, Bergert ER, Myers RM, Harvey ME, Classic KL, Blanco MC, Frisk CS, Marler RJ, Davis BJ, O'Connor MK, Russell SJ, Morris JC. A pre-clinical large animal model of adenovirus-mediated expression of the sodium-iodide symporter for radioiodide imaging and therapy of locally recurrent prostate cancer. *Mol. Ther.* 2005; 12:835–841. [PubMed: 16054438]
155. Merron A, Peerlinck I, Martin-Duque P, Burnet J, Quintanilla M, Mather S, Hingorani M, Harrington K, Iggo R, Vassaux G. SPECT/CT imaging of oncolytic adenovirus propagation in tumours *in vivo* using the Na/I symporter as a reporter gene. *Gene Ther.* 2007; 14:1731–1738. [PubMed: 17960161]
156. Peerlinck I, Merron A, Baril P, Conchon S, Martin-Duque P, Hindorf C, Burnet J, Quintanilla M, Hingorani M, Iggo R, Lemoine NR, Harrington K, Vassaux G. Targeted radionuclide therapy using a Wnt-targeted replicating adenovirus encoding the Na/I symporter. *Clin. Cancer Res.* 2009; 15:6595–6601. [PubMed: 19861465]
157. Dingli D, Peng KW, Harvey ME, Greipp PR, O'Connor MK, Cattaneo R, Morris JC, Russell SJ. Image-guided ra-diotherapy for multiple myeloma using a recombinant measles virus expressing the thyroidal sodium iodide symporter. *Blood.* 2004; 103:1641–1646. [PubMed: 14604966]
158. Hasegawa K, Pham L, O'Connor MK, Federspiel MJ, Russell SJ, Peng KW. Dual therapy of ovarian cancer using measles viruses expressing carcinoembryonic antigen and sodium iodide symporter. *Clin. Cancer Res.* 2006; 12:1868–1875. [PubMed: 16551872]
159. Carlson SK, Classic KL, Hadac EM, Bender CE, Kemp BJ, Lowe VJ, Hoskin TL, Russell SJ. *In vivo* quantitation of intratumoral radioisotope uptake using micro-single photon emission computed tomography/computed tomography. *Mol. Imaging Biol.* 2006; 8:324–332. [PubMed: 17053863]
160. Carlson SK, Classic KL, Hadac EM, Dingli D, Bender CE, Kemp BJ, Russell SJ. Quantitative molecular imaging of viral therapy for pancreatic cancer using an engineered measles virus expressing the sodium-iodide symporter reporter gene. *AJR Am. J. Roentgenol.* 2009; 192:279–287. [PubMed: 19098211]
161. Russell SJ, Peng KW. Measles virus for cancer therapy. *Curr. Top. Microbiol. Immunol.* 2009; 330:213–241. [PubMed: 19203112]
162. Dupertuis YM, Xiao WH, De Tribolet N, Pichard C, Slosman DO, Bischof Delaloye A, Buchegger F. Unlabelled iododeoxyuridine increases the rate of uptake of [125I]iododeoxyuridine in human xenografted glioblastomas. *Eur. J. Nucl. Med. Mol. Imaging.* 2002; 29:499–505. [PubMed: 11914888]
163. O'Hare NJ, Murphy D, Malone JF. Thyroid dosimetry of adult European populations. *Br. J. Radiol.* 1998; 71:535–543. [PubMed: 9691899]

164. Mazzaferri EL, Kloos RT. Clinical review 128: Current approaches to primary therapy for papillary and follicular thyroid cancer. *J. Clin. Endocrinol. Metab.* 2001; 86:1447–1463. [PubMed: 11297567]
165. Vini L, Harmer C. Radioiodine treatment for differentiated thyroid cancer. *Clin. Oncol. (R Coll. Radiol.)*. 2000; 12:365–372. [PubMed: 11202090]
166. Alexander C, Bader JB, Schaefer A, Finke C, Kirsch CM. Intermediate and long-term side effects of high-dose radioiodine therapy for thyroid carcinoma. *J. Nucl. Med.* 1998; 39:1551–1554. [PubMed: 9744341]
167. Benua R, Cicale NR, Sonenberg M, Rawson RW. The relation of radioiodine dosimetry to results and complications in the treatment of metastatic thyroid cancer. *Am. J. Roentgenol. Radium Ther. Nucl. Med.* 1962; 87:171–182.
168. Maxon HR III, Englaro EE, Thomas SR, Hertzberg VS, Hinnefeld JD, Chen LS, Smith H, Cummings D, Aden MD. Radioiodine-131 therapy for well differentiated thyroid cancer -a quantitative radiation dosimetric approach: outcome and validation in 85 patients. *J. Nucl. Med.* 1992; 33:1132–1136. [PubMed: 1597728]
169. Gershengorn MC, Izumi M, Robbins J. Use of lithium as an adjunct to radioiodine therapy of thyroid carcinoma. *J. Clin. Endo-crinol. Metab.* 1976; 42:105–111.
170. Movius, EG.; Robbins, J.; Pierce, LR.; Reynolds, JC.; Keenan, AM.; Phyllaier, MA. The value of lithium in radioiodine therapy of thyroid carcinoma. In: Medeiros-Neto, G.; Gaitan, E., editors. *Frontiers in Thyroidology*. Vol. Vol. 2. New York: Plenum Press; 1996. p. 1269-1272.
171. Koong SS, Reynolds JC, Movius EG, Keenan AM, Ain KB, Lakshmanan MC, Robbins J. Lithium as a potential adjuvant to 131I therapy of metastatic well differentiated thyroid carcinoma. *J. Clin. Endocrinol. Metab.* 1999; 84:912–916. [PubMed: 10084570]
172. Liu YY, van der Pluijm G, Karperien M, Stokkel MP, Pereira AM, Morreau J, Kievit J, Romijn JA, Smit JW. Lithium as adjuvant to radioiodine therapy in differentiated thyroid carcinoma: clinical and *in vitro* studies. *Clin. Endocrinol. (Oxf)*. 2006; 64:617–624. [PubMed: 16712662]
173. Elisei R, Vivaldi A, Ciampi R, Faviana P, Basolo F, Santini F, Traino C, Pacini F, Pinchera A. Treatment with drugs able to reduce iodine efflux significantly increases the intracellular retention time in thyroid cancer cells stably transfected with sodium iodide symporter complementary deoxyribonucleic acid. *J. Clin. Endocrinol. Metab.* 2006; 91:2389–2395.
174. Huang M, Batra RK, Kogai T, Lin YQ, Hershman JM, Lichtenstein A, Sharma S, Zhu LX, Brent GA, Dubinett SM. Ectopic expression of the thyroperoxidase gene augments radioiodide uptake and retention mediated by the sodium iodide symporter in non-small cell lung cancer. *Cancer Gene Ther.* 2001; 8:612–618. [PubMed: 11571539]
175. Boland A, Magnon C, Filetti S, Bidart JM, Schlumberger M, Yeh P, Perricaudet M. Transposition of the thyroid iodide uptake and organification system in nonthyroid tumor cells by adeno-viral vector-mediated gene transfers. *Thyroid.* 2002; 12:19–26. [PubMed: 11838726]
176. Smit JW, Schroder-van der Elst JP, Karperien M, Que I, Stokkel M, van der Heide D, Romijn JA. Iodide kinetics and experimental <sup>131</sup>I therapy in a xenotransplanted human sodium-iodide symporter-transfected human follicular thyroid carcinoma cell line. *J. Clin. Endocrinol. Metab.* 2002; 87:1247–1253. [PubMed: 11889195]
177. Dadachova E, Bouzazhah B, Zuckier LS, Pestell RG. Rhenium-188 as an alternative to Iodine-131 for treatment of breast tumors expressing the sodium/iodide symporter (NIS). *Nucl. Med. Biol.* 2002; 29:13–18. [PubMed: 11786271]
178. Shen DH, Marsee DK, Schaap J, Yang W, Cho JY, Hinkle G, Nagaraja HN, Kloos RT, Barth RF, Jhiang SM. Effects of dose, intervention time, and radionuclide on sodium iodide symporter (NIS)-targeted radionuclide therapy. *Gene Ther.* 2004; 11:161–169. [PubMed: 14712300]
179. Zuckier LS, Dohan O, Li Y, Chang CJ, Carrasco N, Dadachova E. Kinetics of perrhenate uptake and comparative bio-distribution of perrhenate, pertechnetate, and iodide by NaI symporter-expressing tissues *in vivo*. *J. Nucl. Med.* 2004; 45:500–507. [PubMed: 15001694]
180. Dadachova E, Nguyen A, Lin EY, Gnatovskiy L, Lu P, Pollard JW. Treatment with rhenium-188-perrhenate and iodine-131 of NIS-expressing mammary cancer in a mouse model remarkably inhibited tumor growth. *Nucl. Med. Biol.* 2005; 32:695–700. [PubMed: 16243644]

181. Willhauck MJ, Sharif Samani BR, Gildehaus FJ, Wolf I, Senekowitsch-Schmidtke R, Stark HJ, Göke B, Morris JC, Spitzweg C. Application of <sup>188</sup>rhenium as an alternative radionuclide for treatment of prostate cancer after tumor-specific sodium iodide symporter gene expression. *J. Clin. Endocrinol. Metab.* 2007; 92:4451–4458. [PubMed: 17698909]
182. Carlin S, Akabani G, Zalutsky MR. *In vitro* cytotoxicity of (211)At-astatide and (131)I-iodide to glioma tumor cells expressing the sodium/iodide symporter. *J. Nucl. Med.* 2003; 44:1827–1838. [PubMed: 14602867]
183. Petrich T, Quintanilla-Martinez L, Korkmaz Z, Samson E, Helmeke HJ, Meyer GJ, Knapp WH, Pötter E. Effective cancer therapy with the alpha-particle emitter [<sup>211</sup>At]astatine in a mouse model of genetically modified sodium/iodide symporter-expressing tumors. *Clin. Cancer Res.* 2006; 12:1342–1348. [PubMed: 16489092]
184. Spitzweg C, Scholz IV, Bergert ER, Tindall DJ, Young CY, Göke B, Morris JC. Retinoic acid-induced stimulation of sodium iodide symporter expression and cytotoxicity of radioiodine in prostate cancer cells. *Endocrinology.* 2003; 144:3423–3432. [PubMed: 12865321]
185. Lim SJ, Paeng JC, Kim SJ, Kim SY, Lee H, Moon DH. Enhanced expression of adenovirus-mediated sodium iodide symporter gene in MCF-7 breast cancer cells with retinoic acid treatment. *J. Nucl. Med.* 2007; 48:398–404. [PubMed: 17332617]
186. Harrington KJ, Melcher A, Vassaux G, Pandha HS, Vile RG. Exploiting synergies between radiation and oncolytic viruses. *Curr. Opin. Mol. Ther.* 2008; 10:362–370. [PubMed: 18683101]
187. Hingorani M, White CL, Zaidi S, Merron A, Peerlinck I, Gore ME, Nutting CM, Pandha HS, Melcher AA, Vile RG, Vassaux G, Harrington KJ. Radiation-mediated upregulation of gene expression from replication-defective adenoviral vectors: implications for sodium iodide symporter gene therapy. *Clin. Cancer Res.* 2008; 14:4915–4924. [PubMed: 18676766]
188. Hingorani M, White CL, Merron A, Peerlinck I, Gore ME, Slade A, Scott SD, Nutting CM, Pandha HS, Melcher AA, Vile RG, Vassaux G, Harrington KJ. Inhibition of repair of radiation-induced DNA damage enhances gene expression from replication-defective adenoviral vectors. *Cancer Res.* 2008; 68:9771–9778. [PubMed: 19047156]
189. Kassis AI, Adelstein SJ. Radiobiologic principles in radionuclide therapy. *J. Nucl. Med.* 2005; 46(Suppl 1):4S–12S. [PubMed: 15653646]
190. Walicka MA, Vaidyanathan G, Zalutsky MR, Adelstein SJ, Kassis AI. Survival and DNA damage in Chinese hamster V79 cells exposed to alpha particles emitted by DNA-incorporated astatine-211. *Radiat. Res.* 1998; 150:263–268. [PubMed: 9728654]
191. Kassis AI, Harris CR, Adelstein SJ, Ruth TJ, Lambrecht R, Wolf AP. The *in vitro* radiobiology of astatine-211 decay. *Radiat. Res.* 1986; 105:27–36. [PubMed: 3945725]
192. Charlton DE, Kassis AI, Adelstein SJ. A comparison of experimental and calculated survival curves for V79 cells grown as monolayers or in suspension exposed to alpha irradiation from <sup>212</sup>Bi distributed in the growth medium. *Radiat. Prot. Dosim.* 1994; 52:311–315.
193. Dingli D, Russell SJ, Morris JC 3rd. *In vivo* imaging and tumor therapy with the sodium iodide symporter. *J. Cell Biochem.* 2003; 90:1079–1086. [PubMed: 14635183]
194. Barton KN, Tyson D, Stricker H, Lew YS, Heisey G, Koul S, de la Zerda A, Yin FF, Yan H, Nagaraja TN, Randall KA, Jin GK, Fenstermacher JD, Jhiang S, Ho Kim J, Freytag SO, Brown SL. GENIS: gene expression of sodium iodide symporter for noninvasive imaging of gene therapy vectors and quantification of gene expression *in vivo*. *Mol. Ther.* 2003; 8:508–518. [PubMed: 12946325]
195. Barton KN, Stricker H, Brown SL, Elshaikh M, Aref I, Lu M, Pegg J, Zhang Y, Karvelis KC, Siddiqui F, Kim JH, Freytag SO, Movsas B. Phase I study of non-invasive imaging of adenovirus-mediated gene expression in the human prostate. *Mol. Ther.* 2008; 16:1761–1769. [PubMed: 18714306]

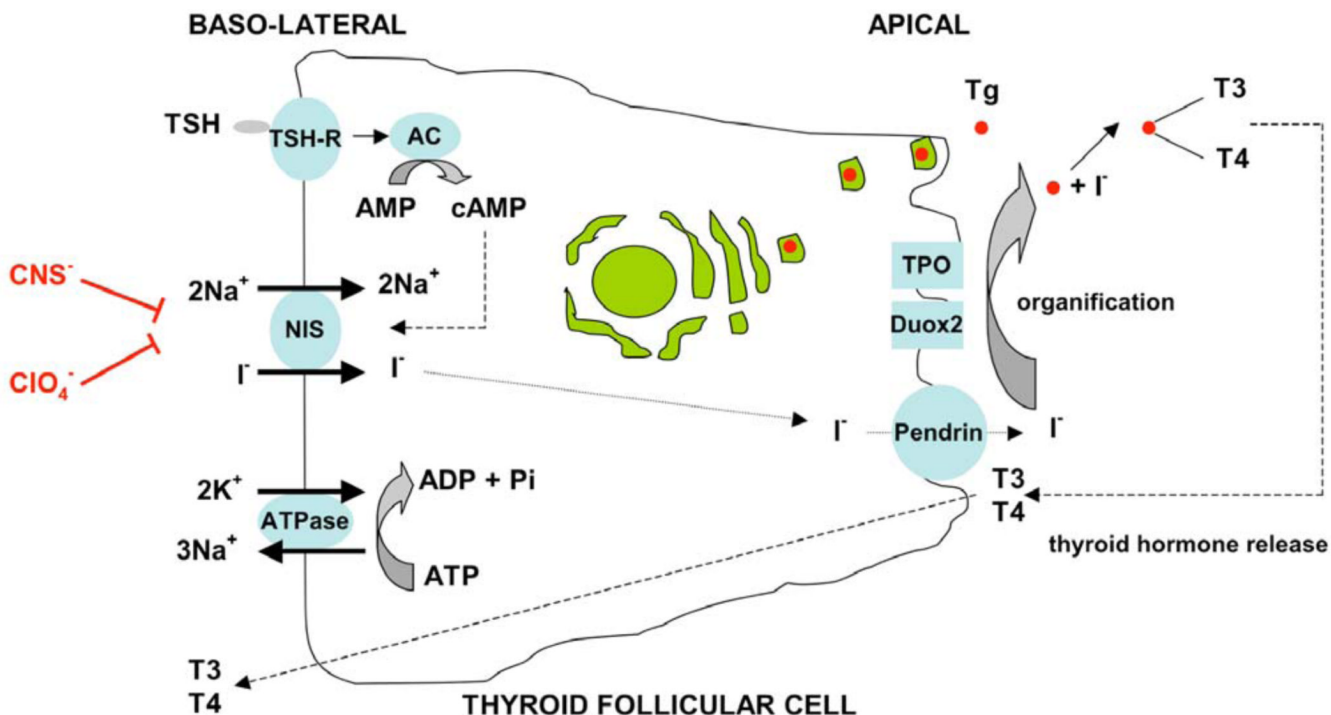


**Fig. 1.** Schematic representation of the role of NIS in iodide transport in normal thyroid follicular cells. Thyroid stimulating hormone (TSH) stimulation of TSH receptor (TSH-R) activates adenylate cyclase (AC) which generates cyclic AMP (cAMP) from AMP. This stimulates NIS-mediated co-transport of two sodium ions along with one iodide ion, with the transmembrane sodium gradient serving as the driving force for iodide uptake. Thiocyanate ( $\text{CNS}^-$ ) and perchlorate ( $\text{ClO}_4^-$ ) are competitive inhibitors of iodide accumulation in the thyroid. The efflux of iodide from the apical membrane to the follicular lumen is driven by pendrin (the Pendred syndrome gene product) and possibly other unknown apical transporters. Iodide organification within the thyroid follicular lumen (mediated by thyroperoxidase (TPO) and dual oxidase 2 (Duox2)) generates iodinated tyrosine residues within the thyroglobulin (Tg) backbone. These are ultimately released as active thyroid hormone (T3 and T4). (Modified from Spitzweg *et al J. Clin. Endocrinol. Metab* **2001** 86, 3327–35).

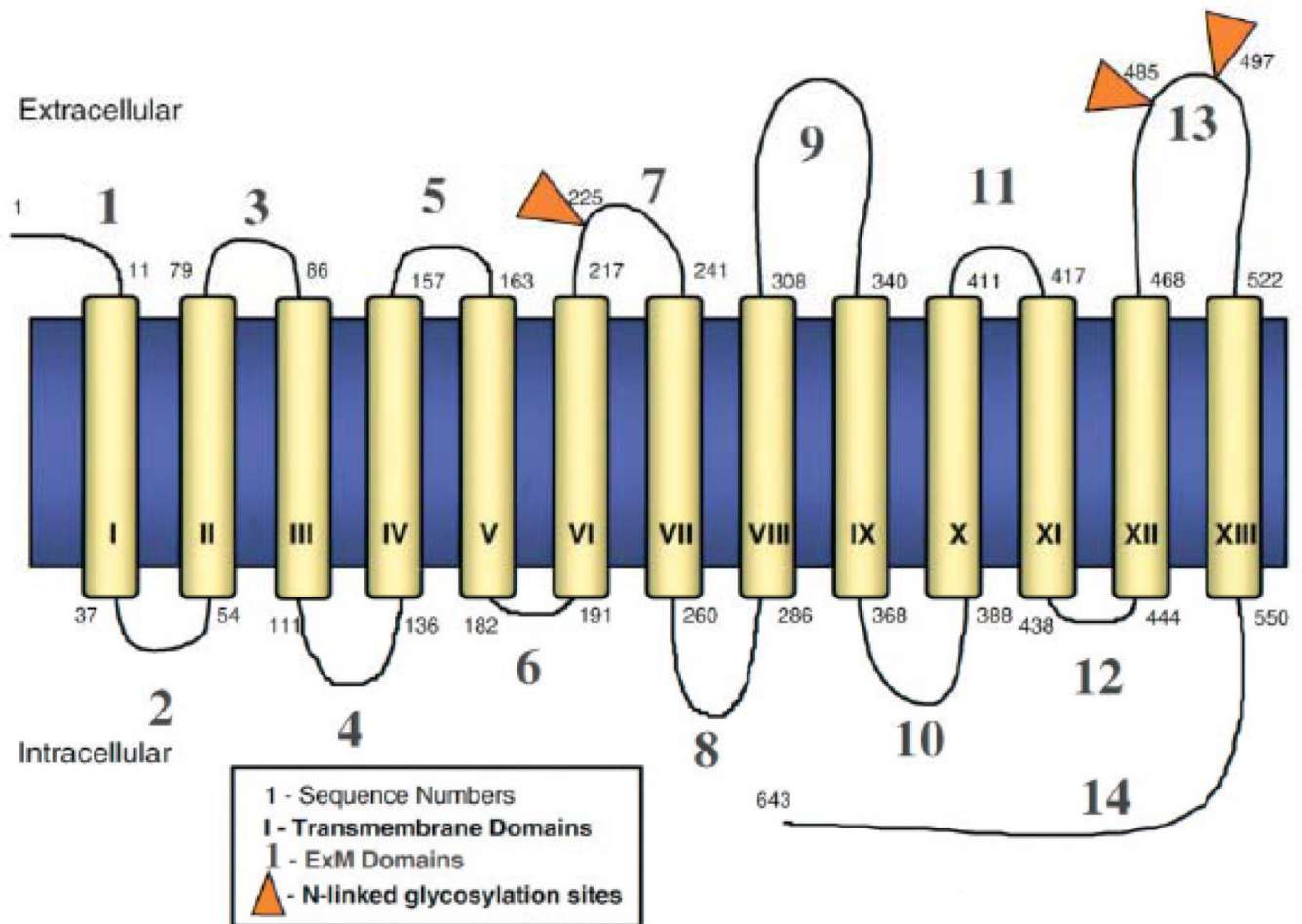


**Fig. 2.** Secondary structure model of functional NIS protein. NIS is predicted to have 13 transmembrane domains with the NH<sub>2</sub> terminus facing extracellularly and the COOH terminus facing intracellularly. There are three potential glycosylation sites at positions 225, 485, and 497 of the amino acid sequence. The length of the 13 transmembrane segments ranges from 20–28 amino acids, except for transmembrane segment V which contains 18 residues. (Modified from Spitzweg *et al J. Clin. Endocrinol. Metab* **2001** 86, 3327–35).

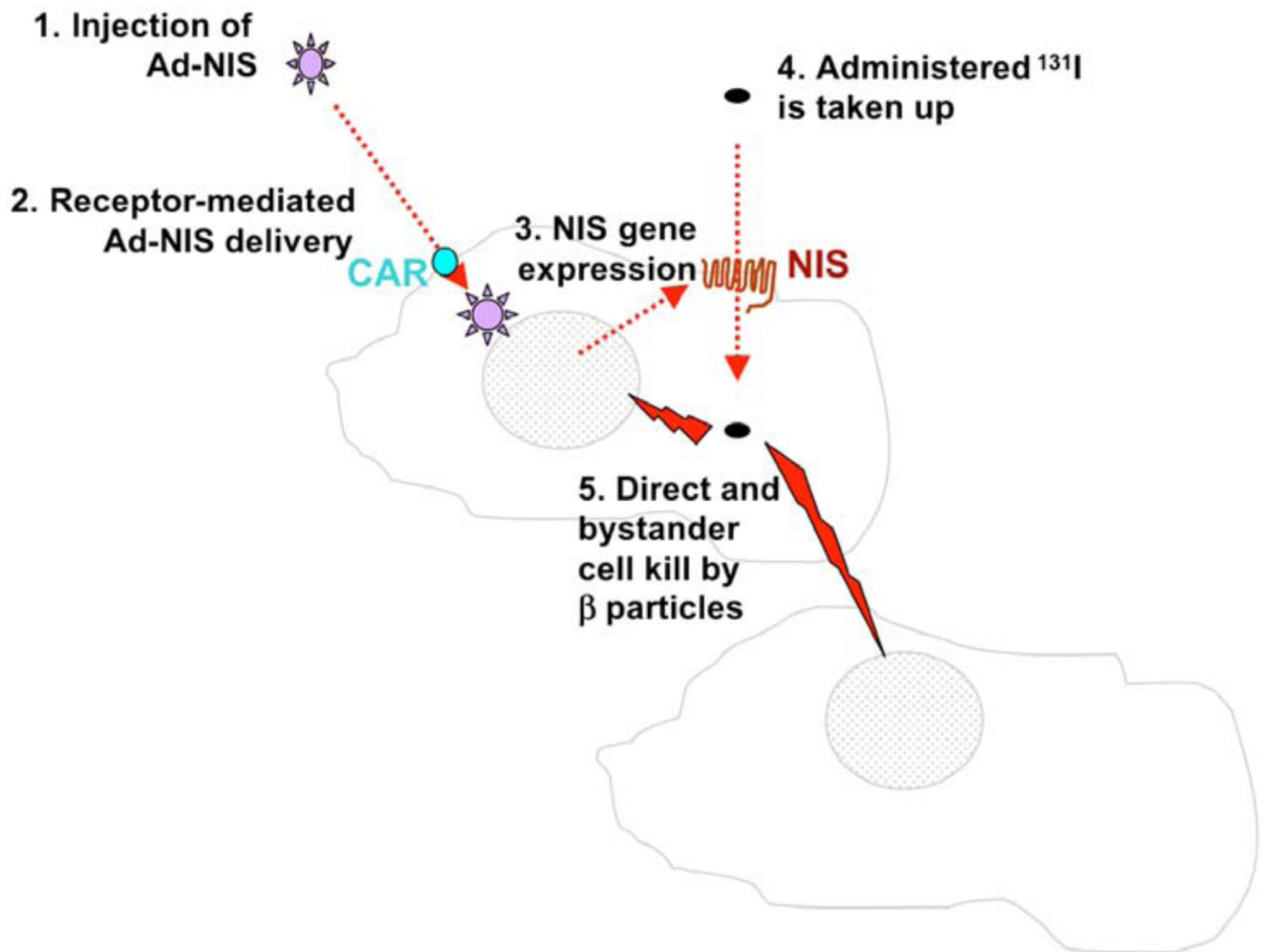


**Fig. 3.**

Schematic diagram of adenovirus-mediated NIS gene delivery: 1. Ad-NIS is injected by the intratumoural, locoregional or systemic route; 2. Ad-NIS infects target cells through the cognate coxsackie and adenovirus receptor (CAR); 3. Ad-NIS drives NIS gene expression and protein is displayed on the cell membrane in infected cells.; 4. Radioiodine is administered systemically and is taken up in NIS-expressing tumour cells; 5.  $\beta$ -particulate radiation mediates both direct and bystander killing of cells.

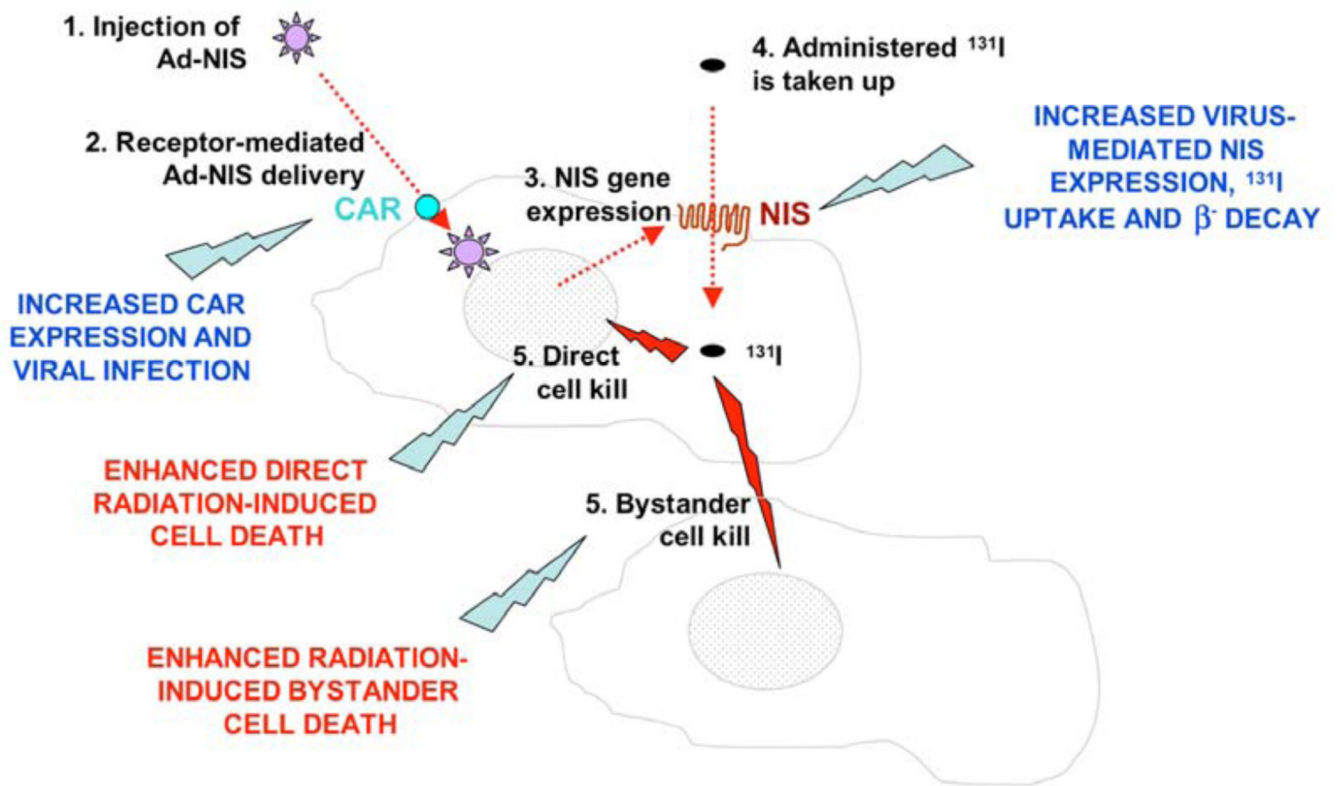


**Fig. 4.** Possible interactions between NIS-mediated radioisotopic therapy and external beam radiotherapy (EBRT). EBRT increases CAR and integrin expression and enhances NIS gene expression from replication-defective adenoviral vectors. The radiation dose delivered via radioiodide, directly to transduced cells and indirectly to bystander cells, can sensitise these cells to the cytotoxic effects of EBRT. Additional use of targeted radiosensitising drugs can lead to further synergistic interactions between radioisotopic irradiation and EBRT.

Table 1

## Pre-Clinical Studies of NIS Gene Therapy

Reference	Study type	NIS delivery	Results
Shimura <i>et al.</i> (1997) [132]	<i>in vitro</i> and <i>in vivo</i> FRTL-Tc cells (thyroid) functional and therapeutic <i>in vivo</i> <sup>131</sup> I dose (1 mCi)	electroporation rNIS cDNA IT injection	restoration of iodide uptake no therapeutic effect
Cho <i>et al.</i> (2000) [134]	<i>in vitro</i> and <i>in vivo</i> U1240 and U251 (gliomas) functional	Adenoviral vectors expressing hNIS regulated by the CMV promoter IT injection	120-fold increase in iodide uptake <i>in vitro</i> 25-fold increase in iodide uptake <i>in vivo</i>
Mandell <i>et al.</i> (1999) [135]	<i>in vitro</i> and <i>in vivo</i> Cell lines: melanoma (A375), liver (BNL.1, ME), colon (CT26), ovarian (IGROV) functional and therapeutic	Retroviral expression of rat NIS (rNIS) (SV40 promoter) IT injection	<i>in vitro</i> therapeutic effect increased iodide uptake (6.9 fold <i>in vivo</i> )
Boland <i>et al.</i> (2000) [136]	<i>in vitro</i> and <i>in vivo</i> Cell lines: cervix (SiHa), prostate (DU145, PC-3), breast (MCF-7 T- 47D), lung (A549), colon cancer functional and therapeutic	Adenoviral vectors expressing rNIS regulated by the CMV promoter IT injection - $2 \times 10^9$ PFU	<i>in vitro</i> therapeutic effect no <i>in vivo</i> therapeutic effect (90 $\mu$ Ci <sup>131</sup> I) increased iodide uptake <i>in vitro</i> (125–225 fold) 11% of <sup>125</sup> I given was recovered per g of infected tumours <i>in vivo</i>
Nakamoto (2000) [137]	<i>in vitro</i> and <i>in vivo</i> breast (MCF-7) functional and therapeutic	electroporation rNIS cDNA	44-fold increase in iodide uptake <i>in vitro</i> retention of <sup>125</sup> I (16.7%) administered <i>in vivo</i>
Spitzweg (2000) [128, 129]	<i>in vitro</i> and <i>in vivo</i> prostate (LNCaP) cancer cell lines functional and therapeutic	Cells stably transfected with hNIS- cDNA (PSA promoter) (NP-1) Adenoviral vectors expressing NIS regulated by the CMV promoter (Ad- CMV-NIS) $3 \times 10^9$ PFU injected IT	perchlorate-sensitive, androgen-driven iodide uptake <i>in vitro</i> therapeutic effect retention of <sup>123</sup> I (25–30%) administered <i>in vivo</i> with biological half-life of 45 hours 90% average tumour volume reduction and 60% complete response (3 mCi <sup>131</sup> I) 80% average tumour volume reduction in viral- transduced tumours (3 mCi <sup>131</sup> I)
Cho (2002) [138]	<i>in vitro</i> and <i>in vivo</i> NIS-transduced glioma cells (F98/hNIS) functional and therapeutic	glioma cells transduced with NIS- expressing retroviral vectors (hNIS (MMV/LTR promoter))	perchlorate-sensitive increase (40-fold) in iodide uptake <i>in vitro</i> NIS-transduced tumours visualised <i>in vivo</i> with <sup>99m</sup> TcO <sub>4</sub> / <sup>123</sup> I scintigraphy radioiodide ( <sup>125</sup> I) retained for upto 24hrs <i>in vivo</i> , biological half-life of 10 hrs improved survival in glioma-bearing rats (F98/hNIS) after 12 mCi of <sup>131</sup> I
Kakinuma (2003) [139]	<i>in vitro</i> prostate (LNCaP), other tumour cell lines (SNU449, MCF-7, HCT116, OVCAR-3, and Panc-1) functional	Adenoviral vectors expressing NIS regulated by the tissue-specific probasin promoter (Ad- ARR(2)PB- hNIS) or the CMV promoter	androgen-dependent, perchlorate-sensitive iodide uptake in LNCaP cells (3.2 fold higher than Ad-CMV-NIS) tissue-specificity of the ARR(2)PB/hNIS con- struct (iodide uptake much lower in non- prostate cell lines)
Seiger (2003) [140]	<i>in vitro</i> and <i>in vivo</i> rat hepatoma functional and therapeutic	rat hepatoma cells stably transfected with hNIS regulated by GT1–1.3 pro- moter (MH3924A)	30-fold increase in iodide uptake <i>in vitro</i> 22-fold increase in iodide uptake <i>in vivo</i> mean dose of 830 mGy delivered to MH3924A xenografts compared with wild-type
Faivre (2004) [142]	<i>in vitro</i> and <i>in vivo</i> rat hepatoma functional and therapeutic	Adenoviral vector expressing rNIS regulated by CMV promoter (Ad- CMV-NIS)	increase in iodide uptake <i>in vitro</i> (non- sustained) increased (20–30% of injected <sup>125</sup> I) and sus- tained iodide uptake <i>in vivo</i> (>11 days) iodide retention <i>in vivo</i> attributed to hepatic

Reference	Study type	NIS delivery	Results
		Intra-portal injection of Ad-CMV-NIS in hepatoma bearing Wistar rats	recycling tumour growth inhibition and regression of tumour nodules <i>in vivo</i>
Gaut (2004) [143]	<i>in vitro</i> and <i>in vivo</i> head and neck (FaDu, SCC-1, SCC-5) functional and therapeutic	Adenoviral vectors expressing NIS regulated by CMV promoter FaDu cells stably transfected with hNIS used for tumour xenografts	perchlorate-sensitive increase in iodide uptake (upto 25-fold) dose-dependent ( <sup>131</sup> I) reduction in <i>in vitro</i> survival <i>in vivo</i> tumour growth delay and regression following <sup>131</sup> I therapy (1 mCi)
Schipper (2003) [144]	<i>in vitro</i> pancreatic neuroendocrine cells (Bon1, QGP) functional and therapeutic	plasmid cDNA (hNIS) regulated by the tumour-specific promoter (chromograninA) or the constitutive (CMV) promoter	20-fold increase in iodide uptake with NIS expression driven by the chromogranin A promoter effective half-life of iodide 5 minutes in QGP and 30 minutes in Bon1 cells marked reduction in clonogenic survival (>99%) following 100 µCi/ml <sup>131</sup> I
Cengic (2005) [145]	<i>in vitro</i> medullary thyroid cancer cells functional and therapeutic	MTC cells stably transfected with hNIS regulated by calcitonin promoter	12-fold increase in iodide uptake in NIS-transduced cell lines Iodide organification (4%) 84% reduction in cell survival with <sup>131</sup> I (0.8 mCi)
Scholz (2005) [146]	<i>in vitro</i> colorectal cancer cells (HCT116) functional and therapeutic	HCT116 cells stably transfected with hNIS regulated by CEA promoter	10-fold increase in iodide uptake in NIS-transduced cells 90% reduction in cell survival with <sup>131</sup> I
Dwyer (2005) [147]	<i>in vitro</i> and <i>in vivo</i> breast cancer: MUC1+ve [T47D], MUC1-ve [MDA-MB-231] functional and therapeutic	Adenoviral vector expressing hNIS regulated by MUC1 promoter (Ad-MUC1-NIS) IT injection – 5 × 10 <sup>8</sup> PFU	58-fold increase in iodide uptake in MUC1+ve [T47D] cells NIS-transduced tumours visualised <i>in vivo</i> with <sup>123</sup> I scintigraphy biological half-life of retained iodide - 5.8hrs <i>in vivo</i> 83% reduction in tumour volume
Dwyer (2006) [148]	<i>in vitro</i> and <i>in vivo</i> pancreatic cancer functional and therapeutic	Adenoviral vector expressing hNIS regulated by MUC1 promoter (Ad-MUC1-NIS)	43-fold increase in iodide uptake <i>in vivo</i> scintigraphy – 13% of injected iodide retained by tumours - optimal uptake at 5 hrs <i>in vivo</i> therapeutic effect with <sup>131</sup> I (>50% reduction in tumour volume) (p<0.0001)
Dwyer (2007) [149]	<i>in vitro</i> and <i>in vivo</i> ovarian cancer functional and therapeutic	Adenoviral vector expressing hNIS regulated by MUC1 promoter (Ad-MUC1-NIS)	5-fold increase in iodide uptake with Ad/MUC1/NIS – compared with 12-fold increase with Ad/CMV/NIS <i>in vivo</i> scintigraphy - less intense uptake with Ad/MUC1/NIS compared with Ad/CMV/NIS <sup>131</sup> I >50% reduction in tumour volume with Ad/CMV/NIS
Chen (2007) [150]	<i>in vitro</i> and <i>in vivo</i> pancreatic cancer (Capan-2 and SW1990) functional and therapeutic	Adenoviral vector expressing hNIS regulated by MUC1 promoter (Ad-MUC1-NIS) IT injection – 5 × 10 <sup>8</sup> PFU	more than 15-fold increase in iodide uptake <i>in vivo</i> with <sup>123</sup> I scintigraphy – 3% retained at 24 hrs biological half-life of 10.5 hrs <i>in vivo</i> therapeutic effect with <sup>131</sup> I (3 mCi) (>75% reduction in tumour volume of NIS-transduced tumours) (p<0.05)
Spitzweg (2007) [151]	<i>in vivo</i> medullary thyroid cancer functional and therapeutic	AV vector expressing hNIS regulated by CEA promoter (Ad-CEA-NIS) IT injection – 5 × 10 <sup>8</sup> PFU	iodide retention of 7.5 ± 1.2% ID/g biological half-life – 6.1 ± 0.8hrs significant reduction in tumour growth with <sup>131</sup> I with reduction in calcitonin levels
Willhauck (2007) [152]	<i>in vitro</i> and <i>in vivo</i> hepatocellular carcinoma functional and therapeutic	stably NIS-transfected murine hepa-1-6 and human hepG2 cell lines	> 75% cell-death following exposure to <sup>131</sup> I hepG2 xenografts accumulated 15% of <sup>123</sup> I biological half-life of 8.4 hours tumour-growth inhibition after 55MBq of <sup>131</sup> I
Dwyer (2005) [153]	<i>in vivo</i> adult male beagle dogs safety and feasibility study	Adenoviral vector expressing hNIS regulated by CMV promoter (Ad-CMV-NIS)	<sup>123</sup> I scintigraphy using SPECT/CT average-absorbed dose of 23 ± 42 cGy after 1 mCi <sup>131</sup> I average-absorbed dose of 1245.1 ± 280.9 cGy

Reference	Study type	NIS delivery	Results
	assessed reporter and possible therapeutic effects of prostatic NIS expression	open intraprostatic injection of $1 \times 10^{12}$ PFU of Ad-CMV-NIS	after 116 mCi/m <sup>2131</sup> I